AN EXPLODING WIRE ION SOURCE

FOR ION IMPLANTATION

By

KENNETH DEAN DUERKSEN

Bachelor of Science

Southwestern State College

Weatherford, Oklahoma

1966

Submitted to the Faculty of the Graduate College
of the Oklahoma State University
in partial fulfillment of the requirements
for the Degree of
MASTER OF SCIENCE
May, 1972

AN EXPLODING WIRE ION SOURCE

FOR ION IMPLANTATION

Thesis Approved:

James Langley
Thesis Adviser

W. A. Sibley

E. E. Kohnke

D. Wunderman
Dean of the Graduate College

ACKNOWLEDGEMENTS

The author wishes to express his deep gratitude to Dr. James Lange who gave direction and encouragement throughout the course of this work. Heinz Hall and the staff of the Physics-Chemistry Machine Shop were very helpful with the design and fabrication of the apparatus. Wayne Adkins was invaluable for the research in doing the glass work on the vacuum system and constructing the various plasma chambers. A note of thanks is given to Mrs. Janet Sallee for excellence in typing the manuscript.

Finally special appreciation is expressed to my wife, Ila, and my son, Kent, for their many sacrifices and infinite patience.

TABLE OF CONTENTS

LIST OF TABLES

LIST OF FIGURES

LIST OF FIGURES (Continued)

CHAPTER I

INTRODUCTION

A. Scope of Study

Early experiments with superconductors containing small concentrations of impurities have shown a marked effect in superconducting properties[1,2]. However, great difficulty is incurred when attempting to introduce some of the ferromagnetic ions such as nickel, cobalt, and iron into lead. Due to the relative high melting point of Ni, Co, and Fe compared to the low boiling point of Pb, the normal diffusion process cannot be used in making thin films and the necessary process of keeping the substrate near $1^{o}K$ while introducing the impurity is cumbersome and complicated[1]. The recently discovered process of ion implantation is a possible solution to the problem of impurity introduction. Since 1965 the technique of ion implantation has grown considerably as a tool in solid state physics[3-11]. A good review of the subject is given by Mayer, et. al.[12]. The typical ion source has a current density of 0.1-1 $\mu A/cm^2$ [13]. This current density integrated over a 15 minute period, the typical implantation time, will dope a crystal to a depth of 0.5 μm at a level of 10^{19} ions/cm^3. For industrial purposes this is an inconveniently long time to wait to have a specimen doped. This, and other undesirable characteristics to be discussed later, led to the design of an Exploding Wire Ion Source for Ion Implantation. This work deals with the design of the apparatus and the study of the ion charac-

teristics. No implantation or superconducting effects were studied. The future study of these effects is the motivation for the undertaking.

B. Exposition of the Exploding Wire Phenomena

To use an exploding wire as an ion source one does not need to determine the mechanism of plasma formation. However, for a better understanding of the plasma, a discussion of the exploding wire phenomenon will be given.

The study of exploding wires began in 1773, but it wasn't until after World War II that serious scientific investigation of the exploding wire phenomena began[14]. Since that time the literature in the field has become extensive[15-18]. Still, the electrically exploded wire is a complex phenomenon which leads to a need for continued research in the field[19]. When a large amount of electrical energy in a capacitor is released into a small wire, the wire explodes. The basic circuit for this process is illustrated in Figure 1. The labels R and L represent the characteristic resistance and inductance of the circuit. If these are made small, the energy is released rapidly allowing for a peak current of 10^4 amps and a peak power on the order of 10^{12} watts[20]. When the wire explodes, a plasma is formed[14]. A number of models for the formation of this plasma exist[14], one of which is a vaporization wave considered by Bennett, Kahl, and Wedemeyer[21]. It is their thesis that an expansion wave propagates in toward the center. This propagation compresses the inner conducting core reducing the cross sectional area and hence increasing the resistance. The conduction process cuts off when the vapor wave front reaches the center. The wire material exists in two states: (1) the conducting material not affected by the

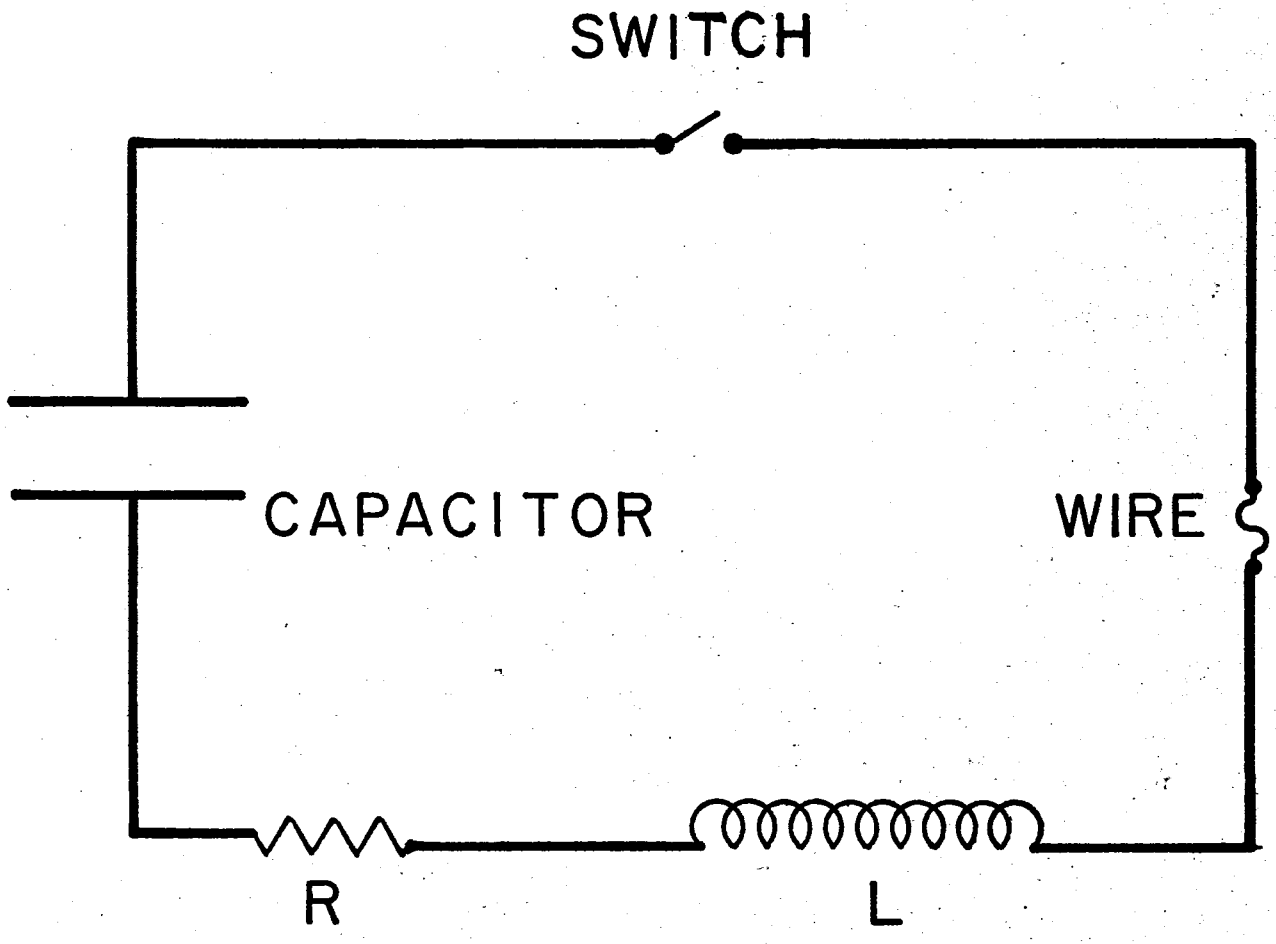

Figure 1. Basic Exploding Wire Circuit

expansion wave and (2) the expanded, nonconducting material behind the wave. A liquid to a wet vapor phase change occurs at the wave front. The compression of the core increases the rate at which energy is dissipated and hence gives rise to high temperatures on the order of $10^4 - 10^5$ ^oK. It should be pointed out that this model does not rely on the pinch effect due to the magnetic field generated by the large current.

Another model is proposed by Ross[22] and Ross and Zinke[23]. Basically this theory assumes initial joule heating of the wire to the melting point, melting and heating, and then superheating the liquid. An electrical breakdown occurs on the outer edge of the superheated liquid. The current passing through the liquid is then switched to the plasma generated by the breakdown. This plasma is compressed around the center core by the magnetic field generated by the current. The heating of the plasma is due to a compressing sheath and an expanding inner core. The flow velocity of the plasma is generated by the interface between the plasma and the expanding core. This theory gives rise to larger temperatures than those reported by Bennett[21]. The basic difference between the two models is the magnetic field dependence in the latter model.

The models presented in the literature are occasionally modified by changing the experimental parameters. Erb and Calker[24] considered nickel, molybdenum, and tungsten wires instead of the commonly used copper and Oktay[25] investigated the effect of wire cross sections. The important fact to note is that a plasma is formed. In general a plasma is a collection of ions with one, two or more elementary charges, molecular ions, neutral atoms, neutral molecules and electrons[26]. The

ions are the point of interest in using an exploding wire for an ion source.

C. A Short Review of Plasma Diagnostics

As has been mentioned, a plasma contains, among other things, positive ions. Two items of great interest are the energy and density of these ions. A number of diagnostic techniques are available for determining one or both of these quantities. One technique is the use of optical spectroscopy. In an optically thin plasma a measurement of the absolute intensity of a spectral line coupled with the atomic transition probability and the plasma dimensions leads to a measure of the positive ion density[27]. Microwave transmission is another well-established method for measuring plasma density[28] since the plasma refractive index depends on the density.

One of the most fundamental techniques--in fact the first one used--for measuring plasma properties is the use of electrostatic probes developed by Langmuir[29]. This technique is discussed in detail by Mott-Smith and Langmuir in a 1926 paper[30]. Francis F. Chen gives an excellent discussion of electrostatic probes in the extensive diagnostics volume edited by Huddlestone and Leonard[31], and other electrostatic probe methods are discussed in the extensive literature[32-36]. Basically an electrostatic probe is a conductor inserted into the plasma which is biased either positively or negatively depending on what species of charge particle is to be observed.

The probes used in the Exploding Wire Ion Generator are similar to those used by Cooney[37] and Ross[22]. The operation of this type of probe is as follows. Two or more electrodes are inserted into the

plasma chamber and a bias voltage (usually 20 to 90V) is applied to them by a capacitor in series with a resistor. As the plasma comes in contact with the electrodes a current flows through the resistor. The resulting voltage drop across the resistor is displayed on an oscilloscope. If two or more probes are used, the system can be used to measure the velocity and hence the energy of the ions. This is the time-of-flight technique of plasma diagnostics. A similar probe method can be used to measure the ion density directly, but it has the disadvantage of sweeping the plasma out of the beam making further use of the ions impossible[38].

D. A Discussion of the Standard Ion Sources

A number of the currently used ion sources were developed for use in accelerators for nuclear physics before ion implantation was a known process. Some of the more common sources are discussed here. The description of others can be found in the literature, see for example Livingston and Blewett[45].

One of the more referenced ion sources is the Magnetic Ion Source used at the Institute for Theoretical Physics in Copenhangen and discussed by K. O. Nielsen[39,40]. Basically this type of ion source operates as follows. The solid material of the desired ion species is placed in a furnace where it is evaporated into the discharge chamber. The geometry of the discharge chamber is such that electrons emitted from a filament are attracted through the vapor to the anode. A 1 kilogauss field surrounding the chamber combined with the cathode - to - anode electric field causes the electrons to move in helical orbits. The electrons then are oscillated between a top and bottom plate which

both act as the cathode. The oscillating electrons cause ionization of the ion species vapor. Hence a plasma is formed which fills the entire chamber. The potential of a plasma depends on the potentials of the surrounding walls. In a discharge chamber in which all the walls have the same potential the plasma potential is so much higher than that of the walls, that the plasma balance is fulfilled. However, in a discharge chamber where the end plates have a different potential from the anode (such as Nielsen's ion chamber) the balance is fulfilled with the plasma potential E_p lower than that of the previous case. Nielsen and Almén[40] assume the plasma potential E_p to be lower than the anode potential E_a. Thus the following type of transition between the end plates occurs. Both plates are negative relative to the plasma. Only a few electrons penetrate this potential difference. Therefore, a region of positive charge is formed near each negative plate. Inside the plasma, between the neutral region and the positive charge, a weak electric field accelerates the ions towards the plasma boundary. The current density through the plasma as referenced by Almén and Nielsen[40] is

$$i^+ \approx n^+ \sqrt{\frac{k\,T_e}{2\pi\,e\,m^+}} \text{ ions/cm}^2 \text{ sec} \qquad (1.1)$$

where n^+ is the density of the plasma, m^+ the mass of an ion in grams, T_e the electron temperature, k is Boltzmann's constant, and $e \approx 2.718$. The plasma boundary follows the electric potential lines which causes a convergence of the ions at the outlet of the chamber where they are then emitted from the chamber as an ion beam. Magnuson, et. al.[41] have described a source which has some desirable characteristics, but it too requires an oven for vaporization of the donor material. The beam cur-

rent of this device is on the average about 60 μA.

Brown and Renton[42] have described a sputter ion source for use with ion implantation in which a gas is introduced into the arc chamber. The beam currents vary from a maximum of 50 μA. A high current source has been described by Krimme[43] and other sources have been described by Wilson[44] and Livingston and Blewett[45].

Almost all of the sources currently in existence have a number of things in common. Some of these are (1) relatively low current levels, (2) the need for large vacuum systems to remove the gas from the beam chamber, and (3) the complexity of construction and operation. Each of these characteristics makes the exploding wire device worth investigating as a source of ions from high melting point solid materials.

CHAPTER II

EXPERIMENTAL APPARATUS AND DATA COLLECTION

A. The Basic System

The basic exploding wire configuration is a typical RLC circuit as illustrated in Figure 2. The capacitor bank C consists of 10 General Electric #18F224 capacitors each of which has a capacitance of 7 μf. Two capacitors are connected in series with five pairs of series capacitors connected in parallel. The bank has a total capacitance of about 17.5 μf and stores 875 joules of energy when charged to a potential of 10 kilovolts. The power supply (labeled PS in Figure 2) is a Capacitor Products number HV100-502M unit. By varying the primary voltage, the unit is capable of continuous DC output from 0 to 10 KV at 5 milliamperes of current. The inductance L is 0.445 μhenries which is the characteristic inductance of the circuit. This inductance was measured in the following way. The resistor R was removed from the circuit and a wire was exploded. The ringing frequency ω_o was measured from the detector oscilloscope trace. The result shown in Equation 2.1 is obtained from RLC circuit theory with R = 0.

$$\omega_o = \sqrt{1/LC} \tag{2.1}$$

Assuming C is the capacitance of the bank alone and measuring ω_o, L is readily obtained. The label R indicates the damping resistor. It was

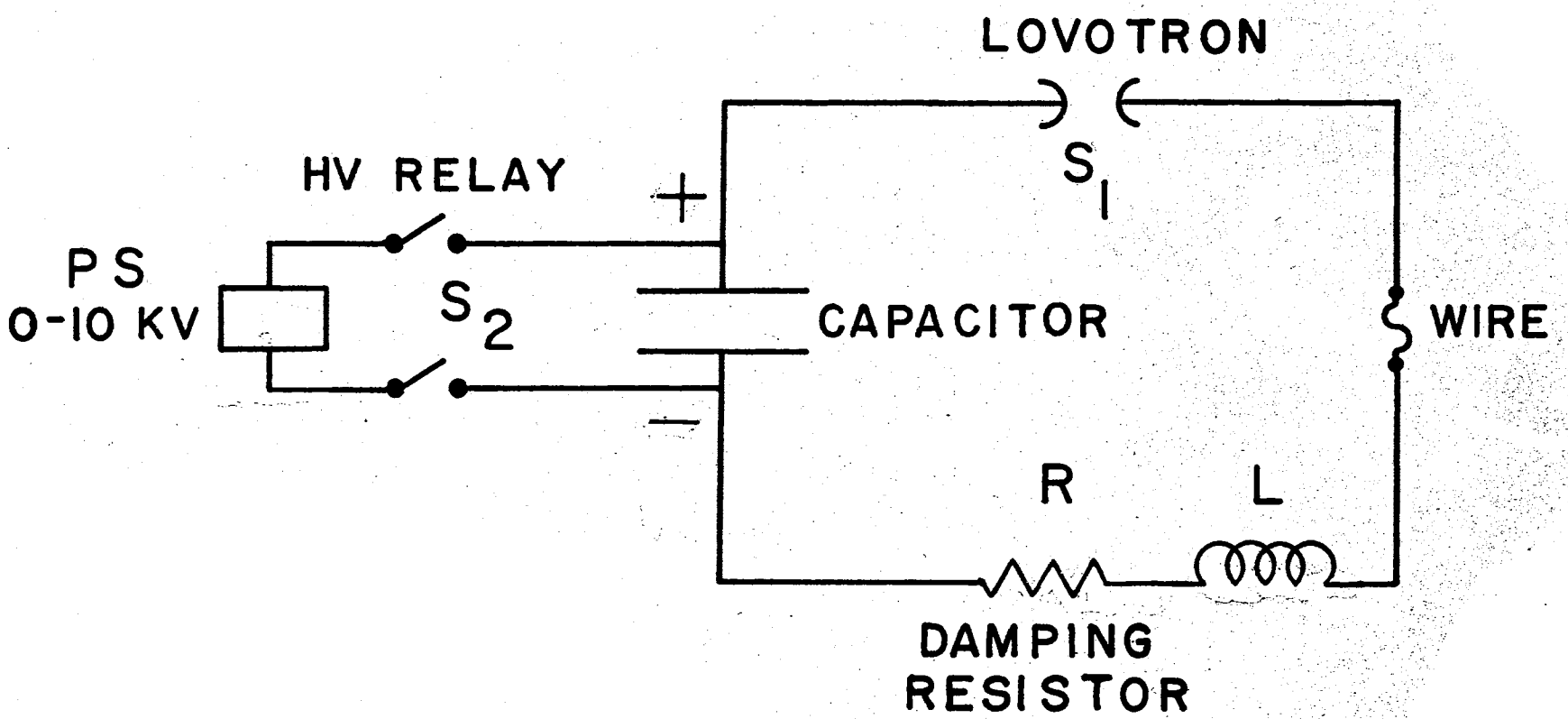

Figure 2. Exploding Wire Circuit Used for Ion Generator

found that measureable results could not be obtained if the circuit were allowed to oscillate. The value of R, which is chosen such that the circuit is slightly underdamped, varies from 0.2 ohms to 0.15 ohms depending on the amount of damping desired. The resistor is constructed from 14 parallel strands of #24 gauge Nickel Chrome Alloy A wire about 15 inches in length. This wire then is bent in the form of an S to shorten the resistor length to 2 inches and still maintain a low inductance. Several resistors where exploded or at least melted before a satisfactory combination could be found. The switches S_2 are normally closed high voltage relays which are opened prior to exploding the wire.

The switch S_1 is a spark gap switch called a Lovotron[46] illustrated in Figure 3. The Lovotron is constructed of two copper rods with the ends formed into a hemisphere. The positive electrode has a 0.187 inch diameter Delrin cylinder in the center which has a 0.060 inch tungsten rod passing through its center. The positive and negative electrodes are spaced a distance about 10% greater than the breakdown gap for the potential used. For 10 KV the experimentally determined gap is 0.138 inches. When the switch is to be activated, a high voltage pulse is applied to the tungsten rod and an arc is struck between the rod and the positive electrode. The resulting ionization causes a breakdown of the gap and the switch conducts. The pulse circuit is illustrated in Figure 4. The high voltage pulse is generated by discharging a 1 μf capacitor through the primary of an automobile ignition coil. The resulting output pulse can reach a potential in excess of 20 KV, however, the discharge is initiated before this potential is reached. This switch has a rise time on the order of several nanoseconds, little or no jitter, and very high current capability.

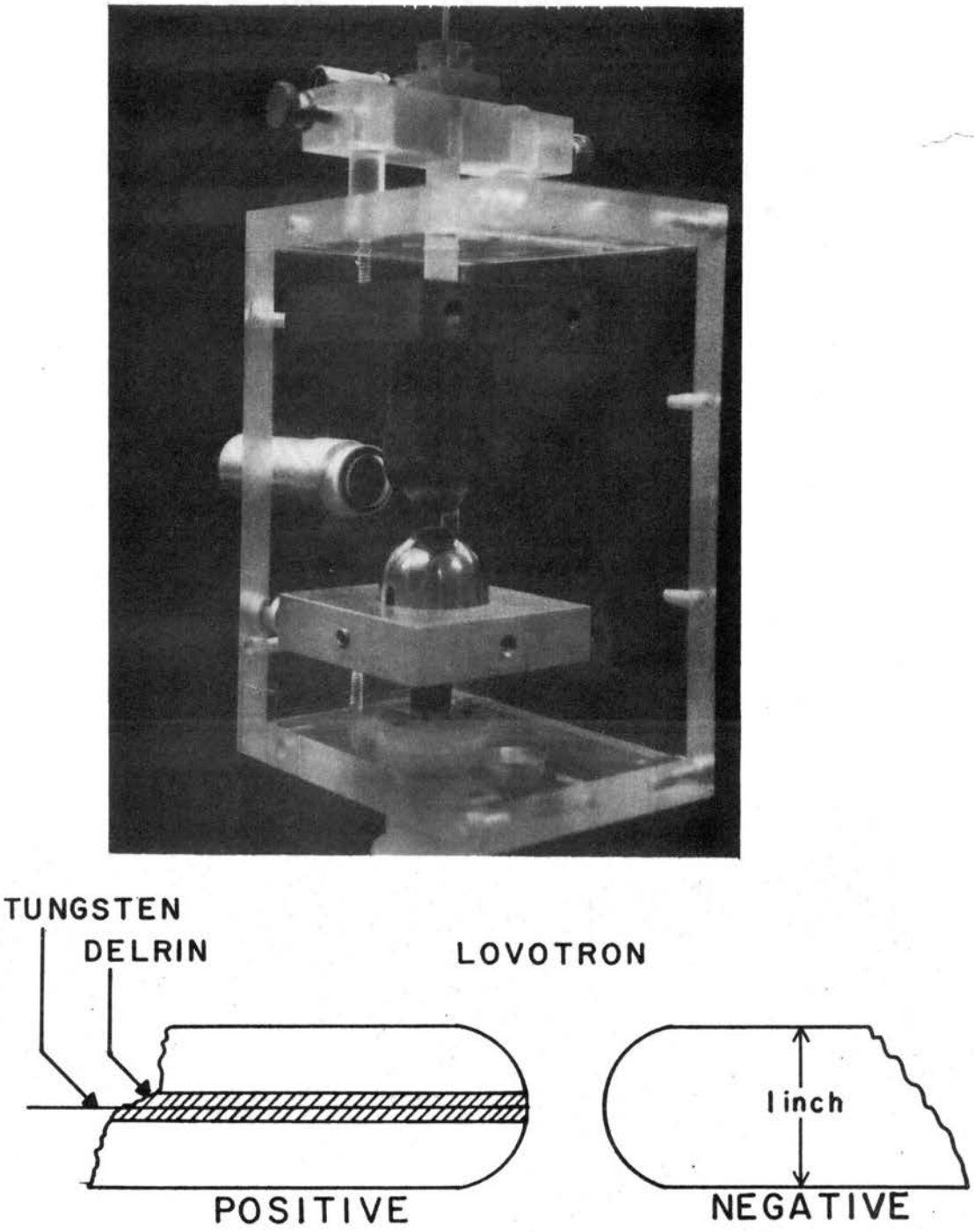

Figure 3. Photograph and Diagram of Lovotron Switch

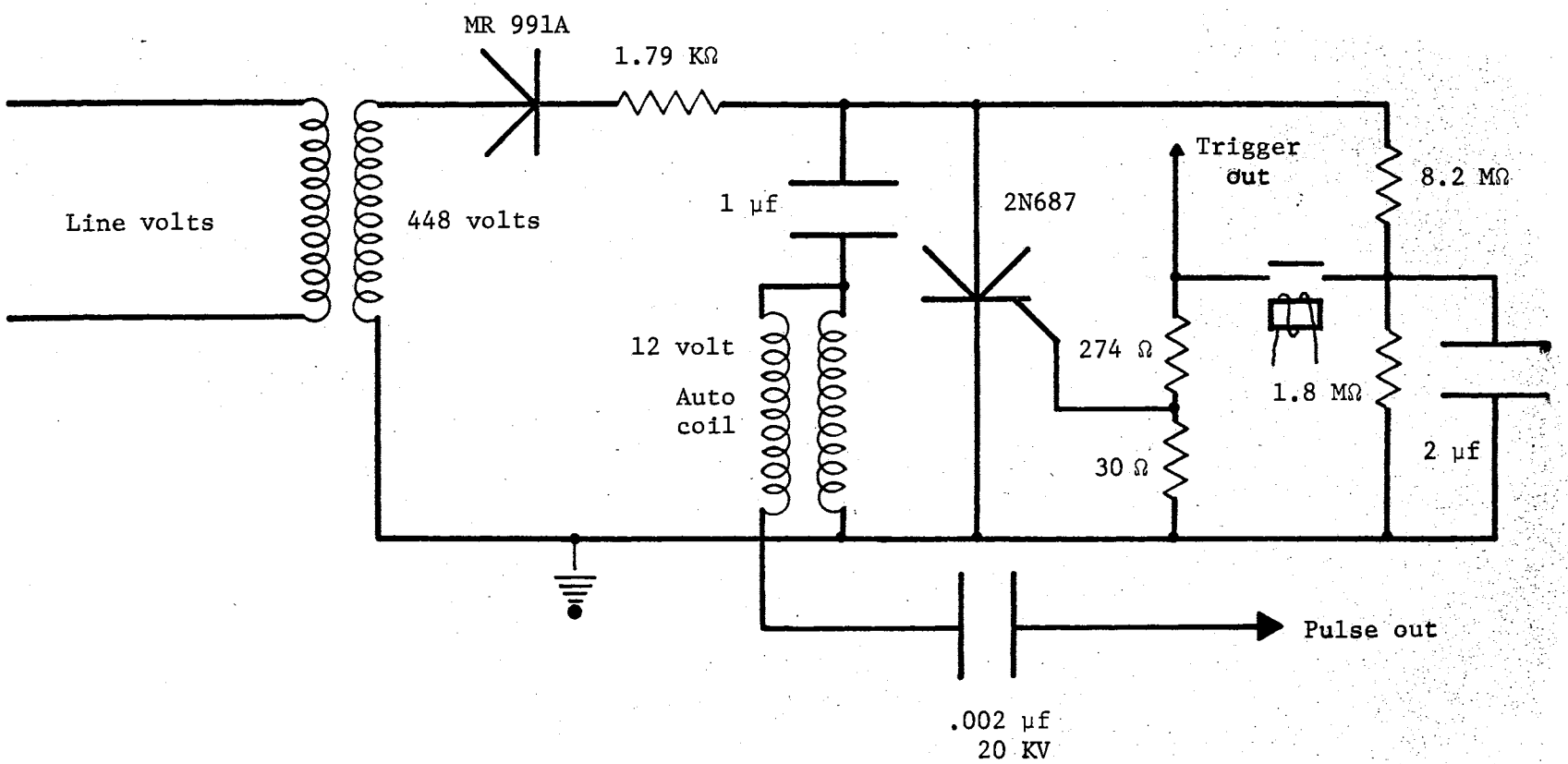

Figure 4. Schematic Diagram of Pulse Circuit

The wire to be exploded is held by two copper clamps which are connected to two copper buss bars 1/2 inch in diameter. This arrangement is seen in Figure 5. One buss bar is connected to the damping resistor and the other buss bar is connected to the switch. The capacitor connections are made by two parallel 2 inch by 1/4 inch copper bars separated by 1/4 inch thick phenolic. Thus the capacitor system is in a low inductance configuration. The buss bars, clamps, and wire form a square loop which is important for plasma acceleration.

The system as a unit can best be described by discussing the procedure for exploding a wire. A wire is placed in the clamps and the chamber is evacuated to about 10^{-6} torr. The safety knife switch is opened and the charge switch is activated. The activation of the charge switch opens a normally closed safety high voltage relay, and it connects the primary of the high voltage supply to 115 volts AC and the primary transformer of the pulse circuit to 115 volts AC. The complete circuit is shown in Figure 6. The variacs in the primary of the high voltage supply are adjusted to the proper high voltage output. When the capacitor bank is charged, the unit is ready to fire. Should data collection need to be terminated for some reason, the "reset-abort switch" is pushed. This switch activates a latching relay which disconnects the primaries of the power supplies and de-energizes the high voltage safety relay discharging the bank through a 60 K ohm 200 watt resistor.

When the wire is to be exploded, the "fire toggle switch" is activated which disconnects the capacitor bank from the power supply via the high voltage relays (S_2 in Figure 2). then the "fire pushbutton" switch is activated at which time the primaries of the power supplies are disconnected from the 115 V AC source. Simultaneously, a voltage pulse

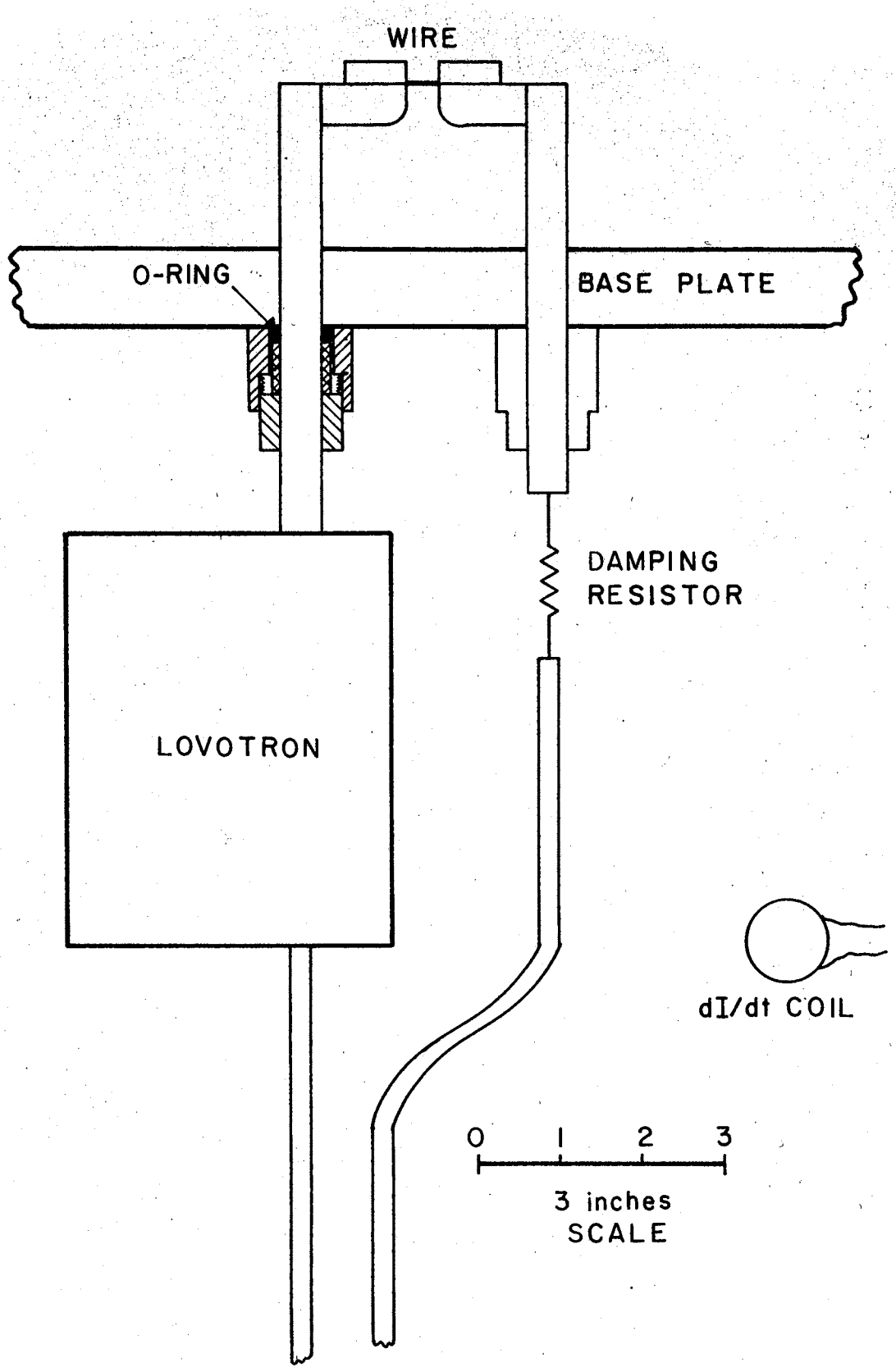

Figure 5. Scale Drawing of Wire Clamps and Buss Bars

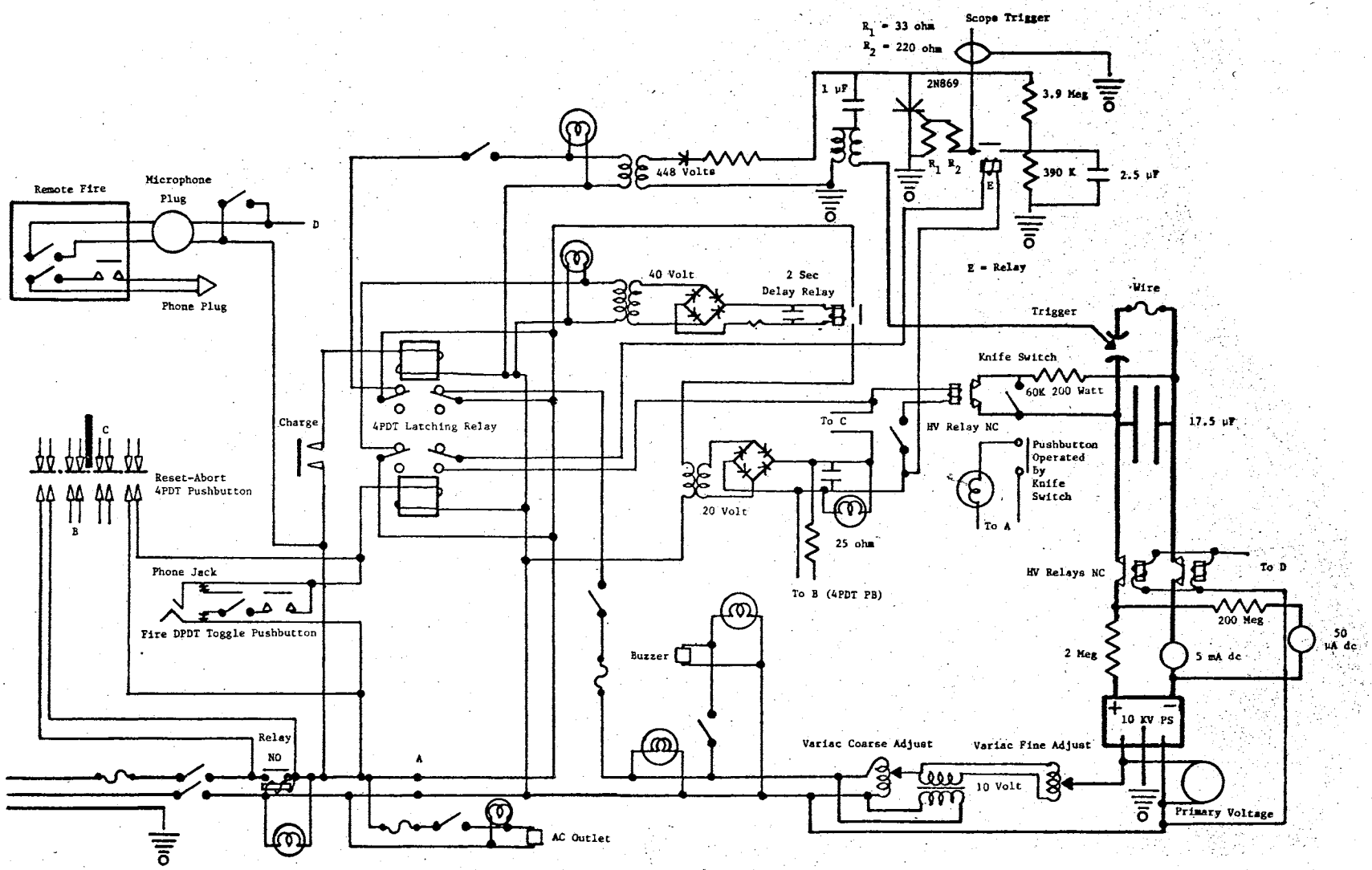

Figure 6. Detailed Schematic Diagram of Exploding Wire Circuit

triggers the oscilloscopes and turns on a silicon controlled rectifier which discharges the 1 μf capacitor into the auto ignition coil. The high voltage pulse then breaks down the gap in the Lovotron and the wire explodes. This system is similar to a system designed by Duerksen, et. al.[47], for use as an aersol generator.

B. The Plasma Probes

A number of different plasma probe configurations have been used with the exploding wire system to determine the effect, if any, of probe design on the flux data. Basically, each one is a biased probe which is a type of Langmuir probe. The probe circuit is labeled flux detector in Figure 7. Three electrodes extend into the plasma. The center electrode is biased a negative 22 volts with respect to the outside two electrodes. Another configuration which gives similar results is to place aluminum foil around the outside of the glass plasma chamber. The three detectors were then biased a negative 22 volts with respect to the foil. A third configuration was formed from 2 copper wire rings, one being 90 mm in diameter and the other 80 mm in diameter. The smaller ring was placed 1/4 inch above the larger. The oscilloscopes record the voltage drop across a resistor which registers the current in the prode circuit due to the plasma. The traces, which are photographed on Polaroid film, are initiated (by the circuitry) about 17 μsec before the wire explodes. In this way one is assured that all of the signal can be recorded since the timing of the triggers can be affected by the proximity of high current discharges.

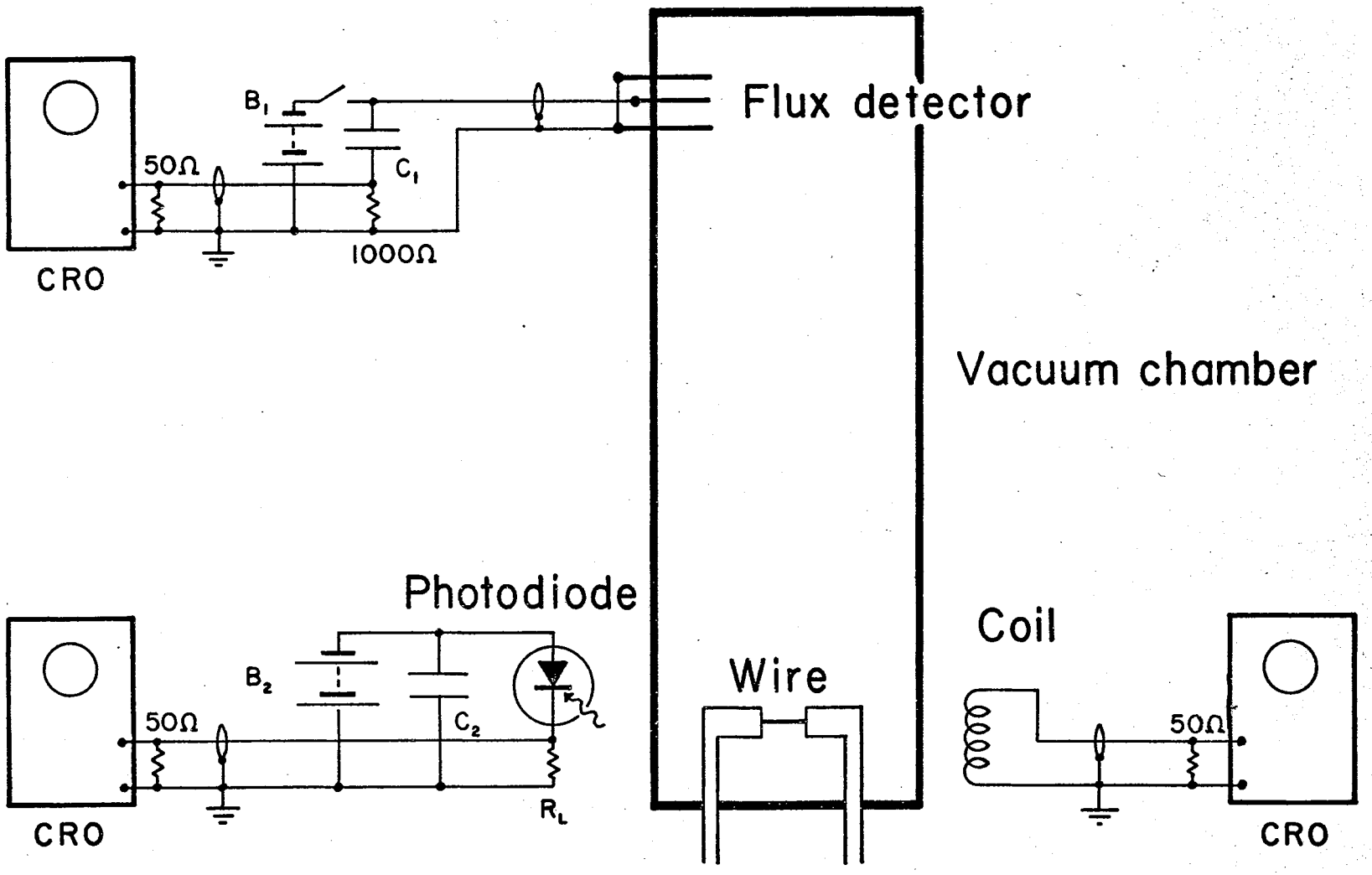

Figure 7. Data Procurement Circuits

C. The Photodiode Circuit

The light from the exploding wire is measured as a function of time using an EG & G SGD 040 photodiode. The circuit for this device is also shown in Figure 7. The bias potential for the device is provided by a 22½ volt battery. A number of different load resistors were used with a 1 Kohm resistor giving the maximum output signal. The SGD 040 can be calibrated to yield an absolute spectral response from 0.35 microns to 1.0 micron wavelength with a maximum response at 0.9 microns. The response time is about 3×10^{-9} sec with response linearity being linear within 5% over seven decades. The field-of-view of this device is 160^{o} making a collimator necessary to avoid signals from plasma which has traveled some distance up the chamber. The data recorded by the oscilloscope is the voltage drop across the load resistor with the scope being triggered by the same method as the flux detectors.

D. The dI/dt Circuit

The change in current as a function of time is measured using a 1 inch diameter coil made of 7 turns of #24 copper wire. This circuit is shown in Figure 7. The coil is placed 2¼ inches away from the negative buss bar and 3 inches below the damping resistor. The current in the buss bar gives rise to a magnetic field which in turn induces a voltage in the coil. This voltage is displayed on an oscilloscope by the same method used for the flux and the photodiode signals. The data from this coil will be used in Chapter III to calculate the current in the discharge.

E. The Plasma Chamber

The plasma chamber is illustrated in Figures 8 and 9. The baseplate is a 1 inch thick piece of plexiglass 12 inches in diameter with the holes around the copper rods made vacuum tight by an O-ring system. The lower part of the chamber is 6 inch I.D. Kimax tempered glass process pipe 18 inches long topped by a 3/4 inch thick piece of plexiglass. Atop this plate stands a 2 inch I.D. Kimax tempered glass process pipe about 4 inches long which is connected to a piece of 3 inch O.D. pyrex glass tube 56 inches long. The detectors are inserted into this last pipe through holes 33½ inches (85 cm) apart with the lower ones 8½ inches above the plexiglass plate. The holes are made vacuum tight with Torr Seal manufactured by the Varian Vacuum Division. The 85 cm distance is used in the time-of-flight analysis. The chamber is pumped with a CVC Model GF26 glass diffusion pump which is backed by a Welch 1402 forepump. To replace a wire, the plasma chamber is isolated from the pump by a VIC 2 inch toggle valve. The effect of the physical dimensions of the plasma chamber and the geometry of the detectors was investigated. To facilitate this investigation a second pipe was also used atop the 2 inch Kimax pipe. This pipe has an outside diameter of 95 mm and a length of 165 mm. The detectors in this pipe are made from #20 copper wire formed into circles, one of which has a 90 mm diameter and the other a 80 mm diameter. The 90 mm diameter is the bottom ring with the 80 mm diameter ring 1/4 inch about it. Two pairs of rings form the two detectors 91.44 cm apart with the bottom one 81.28 cm above the wire.

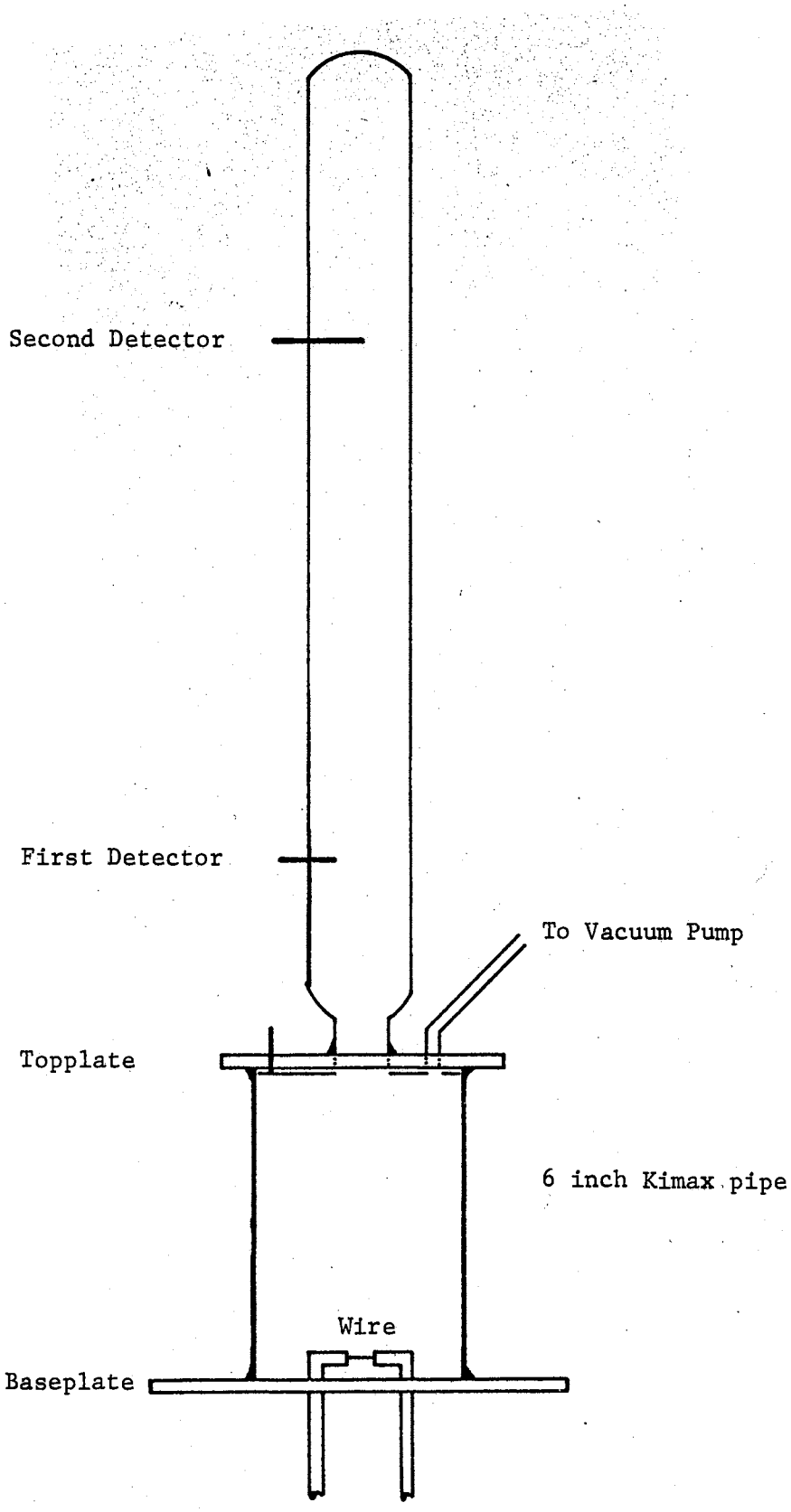

Figure 8. Plasma Chamber

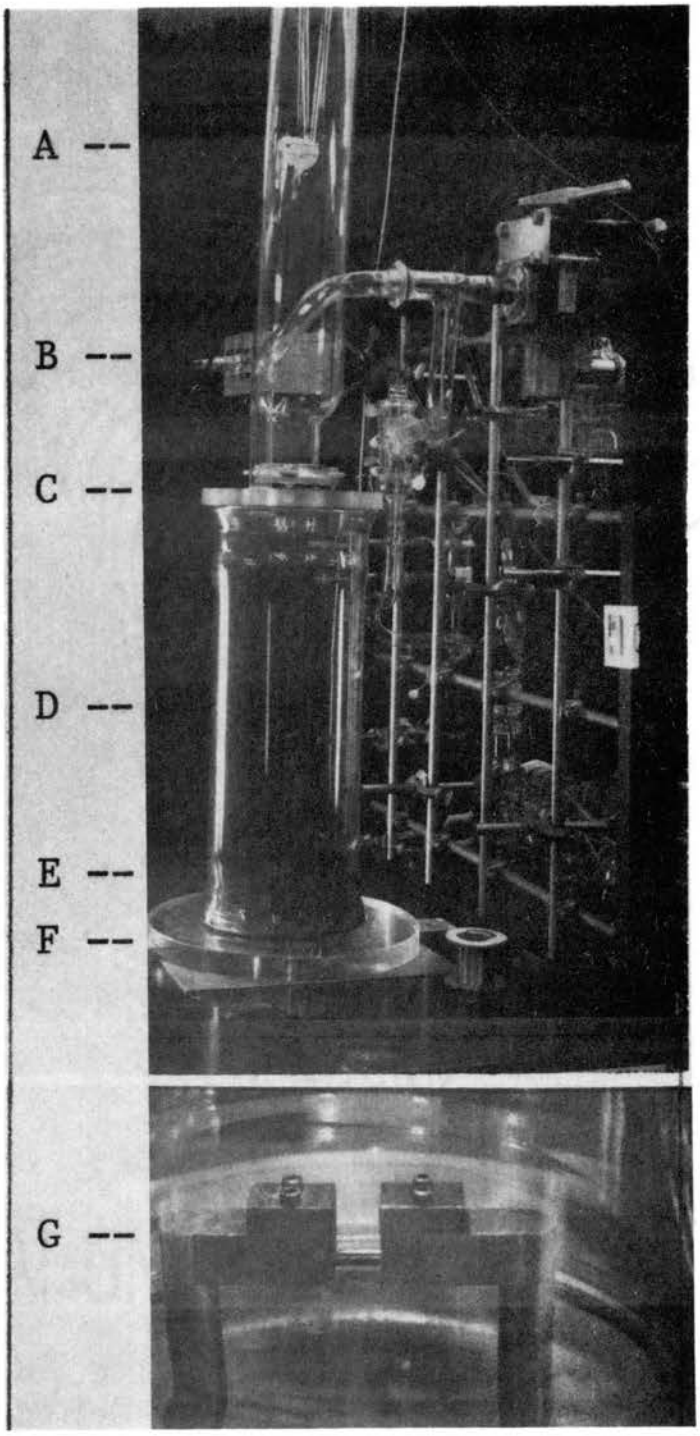

Figure 9. Photograph of Plasma Chamber and Wire Clamps. (A) First Detector, (B) Detector Circuit Box, (C) Top Plexiglas Plate, (D) 6 inch Pyrex Pipe, (E) Wire Clamps, (F) Plexiglas Baseplate, (G) Close-up of Wire Clamps.

CHAPTER III

PRESENTATION OF RESULTS

A. The Acceleration of the Plasma

It has been established from exploding wire theory as discussed in Chapter I that when a wire explodes a plasma is formed. This plasma when formed is accelerated outward from the loop formed by the wire holding electrodes. Figure 10A is a picture of the number 44 wire explosion taken with a Polaroid 110A. By use of a mirror positioned at 45^{o} with respect to the axis of the wire both the transverse and longitudinal views of the plasma can be seen. The camera lens is 41 inches above the floor, 36 inches from the wire, and the lens opening is f90. In this picture a 5 mil nickel wire was exploded at 10 KV in a vacuum of 2×10^{-5} torr. Notice both views show the plasma cloud moving in an upward direction. Figure 10B shows the number 247 wire explosion. Here a 5 mil nickel wire was exploded at 10 KV in a vacuum of 1.9×10^{-6} torr. The camera is 51 inches above the floor, 36 inches from the wire, and the lens opening is f90. Again, as the multiple reflections show, the plasma is accelerated upward. Figure 10C shows a close-up view of the number 229 wire explosion. The camera is 6 inches from the wire, 38½ inches above the floor, and the opening is f45. In addition to the closeup lens, two polarizers were attached to the camera in which their relative orientations were such that 25% of the light was transmitted through the lens.

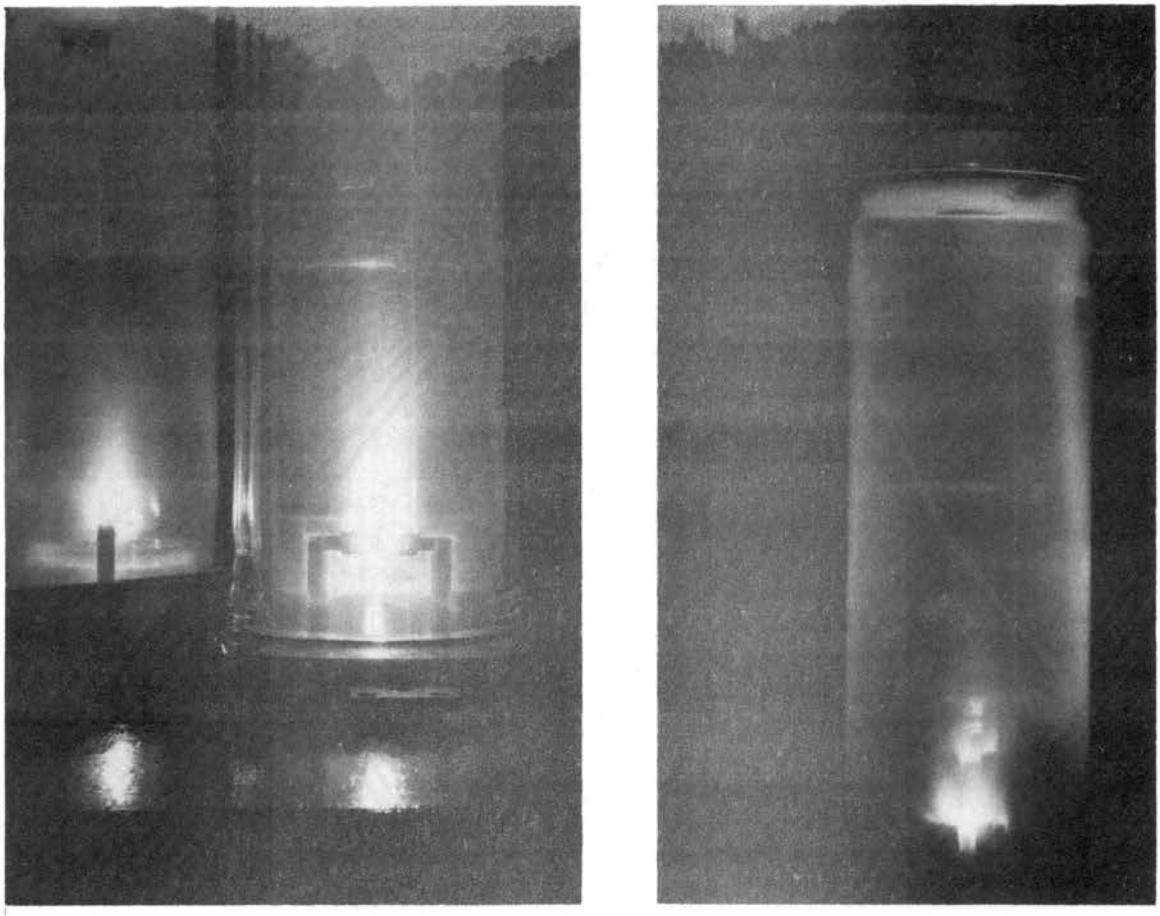

A

B

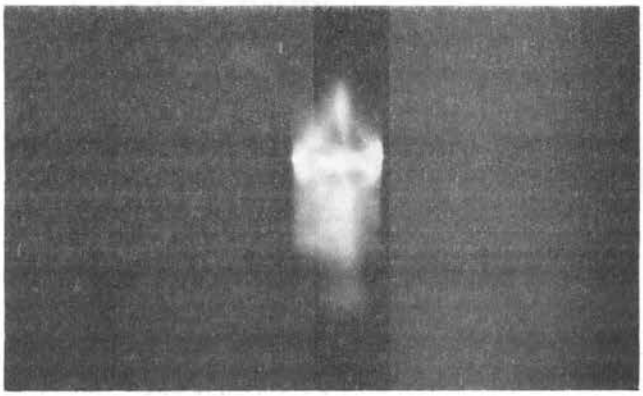

C

Figure 10. Pictures of Wires Exploding

In Chapter I, one possible explanation of the plasma acceleration was presented in the discussion of Ross's model. Here a primitive explanation is given for two sources of the accelerating force. Part of the acceleration can be contributed to the $\vec{J} \times \vec{B}$ force. This can be seen in Figure 11A. The x's represent the magnetic field going into the plane of the electrodes. It can be seen that as one travels around the loop in the direction of I, the flux concentration is less outside the top of the loop than inside. Hence, at the top of the loop there is a net magnetic field coming out of the plane of the electrodes. This net field exerts a $\vec{J} \times \vec{B}$ force upward on the ions. The picture is not as simple as this due to the changing of $\vec{J}$ and $\vec{B}$ with time. But the value of $\vec{B}$ depends on $\vec{J}$ so they change at the same rate. If the ions are released at the current maximum, then $\vec{B}$ would be at its maximum and the ions would be given a net impulse out of the loop. This is known as the kink instability in plasma physics[48].

Furthermore, a net field $\vec{B}$ coming out of the plane of the electrodes exists at the center of the wire. Consider Figure 11B. From the Biot-Savart law

$$\vec{B} = \frac{\mu_o I}{4\pi} \int \frac{\vec{dl} \times (-\vec{r})}{r^3} \tag{3.1}$$

Here a $-\vec{r}$ is used because the vector $\vec{r}$ is considered from the point of interest to the current loop. If one considers the z component of $\vec{B}$ due to the current in one of the electrodes, the integral becomes

$$B_z(o) = \frac{\mu_o I}{4\pi} \int_o^{-\pi/2} - \frac{d/2}{r^2} dy \tag{3.2}$$

where d is the distance between the buss bars and $\vec{dl} \times (-\vec{r}) = (-) dl_y r_x =$

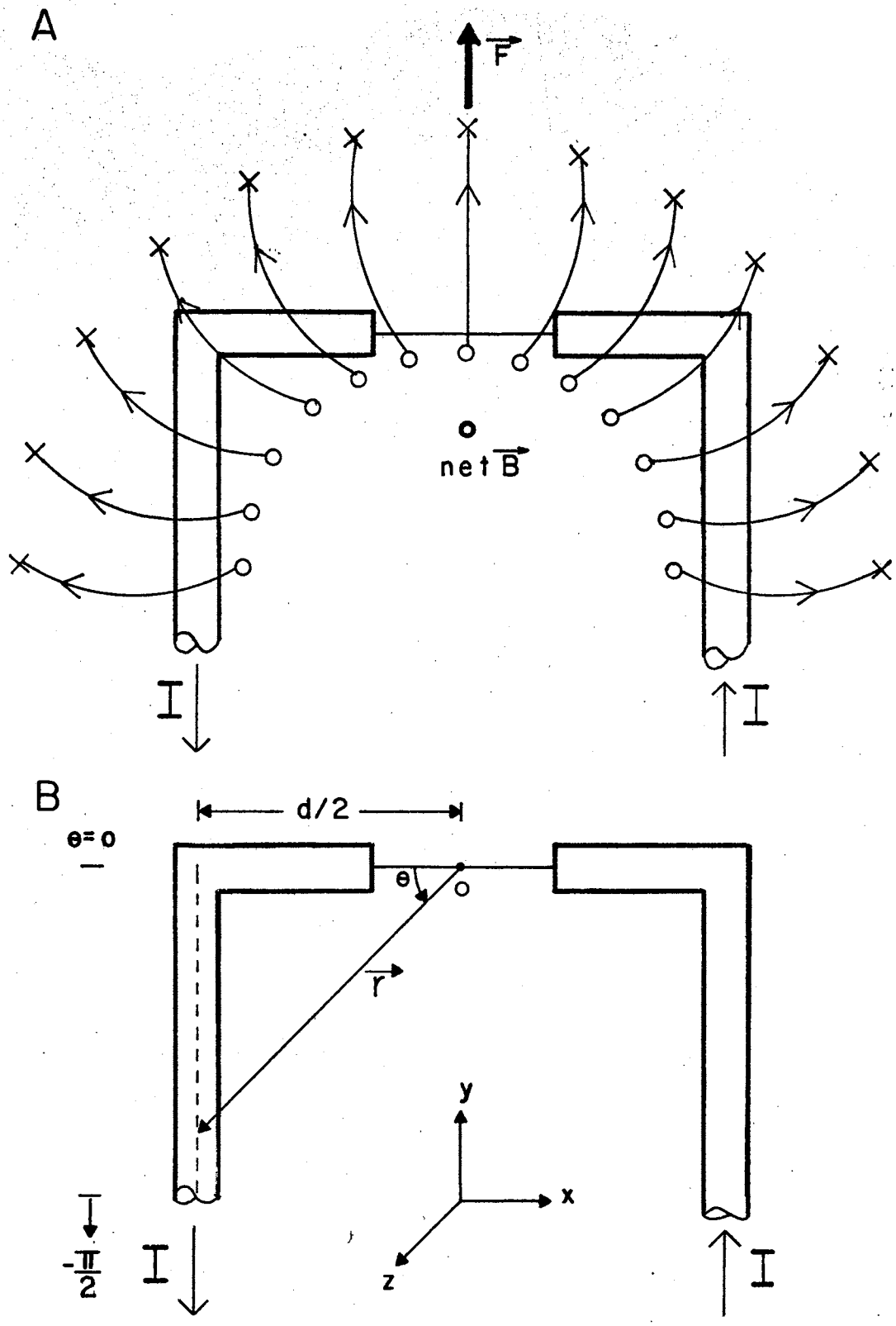

Figure 11. Source of Accelerating Force

-dy d/2. Since $1/r = \cos\theta/(d/2)$ then $(1/r)^3 = \cos^3\theta/(d^3/8)$. Furthermore, $y = (d/2)(\sin\theta/\cos\theta) = d/2 \tan\theta$. Thus $dy = d/2 \sec^2\theta\, d\theta$ and the integral becomes

$$B_z(o) = \frac{\mu_o I}{4\pi}\frac{2}{d}(-)\int_o^{-\pi/2} -\cos\theta\, d\theta \qquad (3.3)$$

Therefore, $B_z(o) = \frac{\mu_o I}{2\pi d}$. By symmetry a similar contribution is obtained from the other side. Thus the total value of B at O is $\mu_o I/\pi d$. Thus in addition to the $\vec{J} \times \vec{B}$ force from the instability there exists a $\vec{J} \times \vec{B}$ from the current in the side electrodes. These two forces are not independent, of course, but this is a primitive explanation for the acceleration upward of the plasma.

B. Calculation of Peak Current and Results of Induction Coil Measurement

The outline of the peak current calculation follows from a straightforward application of RLC circuit theory. First the basic equation is solved to get a solution for I, the current, and ω, the frequency of oscillation. Experimentally ω_o is the measured quantity thus it is assumed that R = 0 and the equations are solved for ω_o. Then I_o, the maximum current when R = 0, is obtained from an energy equation. A combination of the above quantities leads to I_{max}, the maximum current. From RLC circuit theory it is known that

$$RI = -L\frac{dI}{dt} - \frac{q}{C} \qquad (3.4)$$

where R is the resistance, I the current, L the inductance, q the charge,

and C is the capacitance. Taking the time derivative of Equation 3.4 and replacing dq/dt by I one gets the result

$$Ld^2I/dt^2 + RdI/dt + \frac{1}{C} I = 0 . \tag{3.5}$$

Equation 3.5 has the solution

$$I = I_o e^{-\gamma t} \sin (\omega t + \alpha) \tag{3.5a}$$

where

$$\gamma = R/2L \tag{3.6}$$

and

$$\omega = (1/LC - R^2/4L^2)^{\frac{1}{2}} \tag{3.7}$$

Here ω is the frequency of oscillation of the critically damped circuit. Because of the changing resistance as the current increased, ω is difficult to measure experimentally. The frequency of oscillation of the undamped circuit, ω_o, was readily obtained from experiment. Thus, removing the damping resistor from the circuit and letting R = 0 Equation 3.4 becomes

$$\frac{q}{C} = - L \frac{dI}{dt} \tag{3.8}$$

or

$$L\, d^2I/dt^2 + \frac{1}{C} I = 0 . \tag{3.9}$$

This has the solution

$$I = I_o \sin(\omega_o t) \tag{3.10}$$

where the frequency of oscillation is $\omega_o = \sqrt{1/LC}$. Knowing C and measuring ω_o (see Chapter II), L is readily obtained. Now if one assumes that during the oscillation of the undamped circuit that the maximum energy stored in the capacitor is eventually stored in the inductor when the capacitor voltage is zero, one gets

$$\frac{1}{2} C V_o^2 = \frac{1}{2} L I_o^2 . \tag{3.11}$$

Thus

$$I_o = \left(\frac{C V_o^2}{L}\right)^{\frac{1}{2}} . \tag{3.12}$$

Now, as was mentioned in Chapter II, L was calculated by measuring ω_o and found to be 4.45×10^{-7} henries. Thus with $C = 17.5 \times 10^{-6}$ farad, $V = 1 \times 10^{4}$ volts and $L = 4.45 \times 10^{-7}$ henries

$$I_o = 6.28 \times 10^{4} \text{ amp} \tag{3.13}$$

Thus in Equation 3.5a I_o is known. The remaining quantities needed are γt and $\sin \omega t$. From Equations 3.6 and 3.7

$$\omega/\gamma = (4L/R^2C - 1)^{\frac{1}{2}} \tag{3.14}$$

where R is now assumed to be the damping resistor. For this calculation R was measured using a General Radio Bridge to be 1.53×10^{-1} ohms. Since L and C are known

$$\omega/\gamma = 1.83 . \tag{3.15}$$

The quantity of interest, I_{max}, is obtained by taking the time derivative of Equation 3.5a and setting it equal to zero. The result leads to

$$\omega/\gamma = \tan \omega t \, . \tag{3.16}$$

From Equations 3.6 and 3.15 ω can be obtained; from Equations 3.15, 3.16 and ω, ωt and t can be obtained. Thus, I_o, γ, t and ωt, which are known, together with Equation 3.5a yields the current

$$I_{max} = I_o e^{-\gamma t} \sin (\omega t) = 3.17 \times 10^4 \text{ amps} \tag{3.17}$$

for the damped circuit.

The current was measured in another way. Figure 12 shows the results of the measurement of dI/dt using the pickup coil for the number 223 explosion. Point A, the point of ignition, is the point at which the switch begins to conduct current (see Chapter II). The distance AC is the time t_1 and the distance AB is the time called t_2. The quantity, γt_2 is a measure of the attenuation and is equal to ln E/D, where E is the maximum value of dI/dt before I_{max} and D is the maximum value of dI/dt after I_{max}. Now one can see from the figure that

$$\gamma t_1 = \frac{1}{2} \gamma t_2 \tag{3.18}$$

is a good approximation. The quantity γt_1 is the damping factor which limits I_{max}. Thus

$$\alpha t_1 = \frac{1}{2} \ln \frac{E}{D} \tag{3.19}$$

which for Figure 12 is

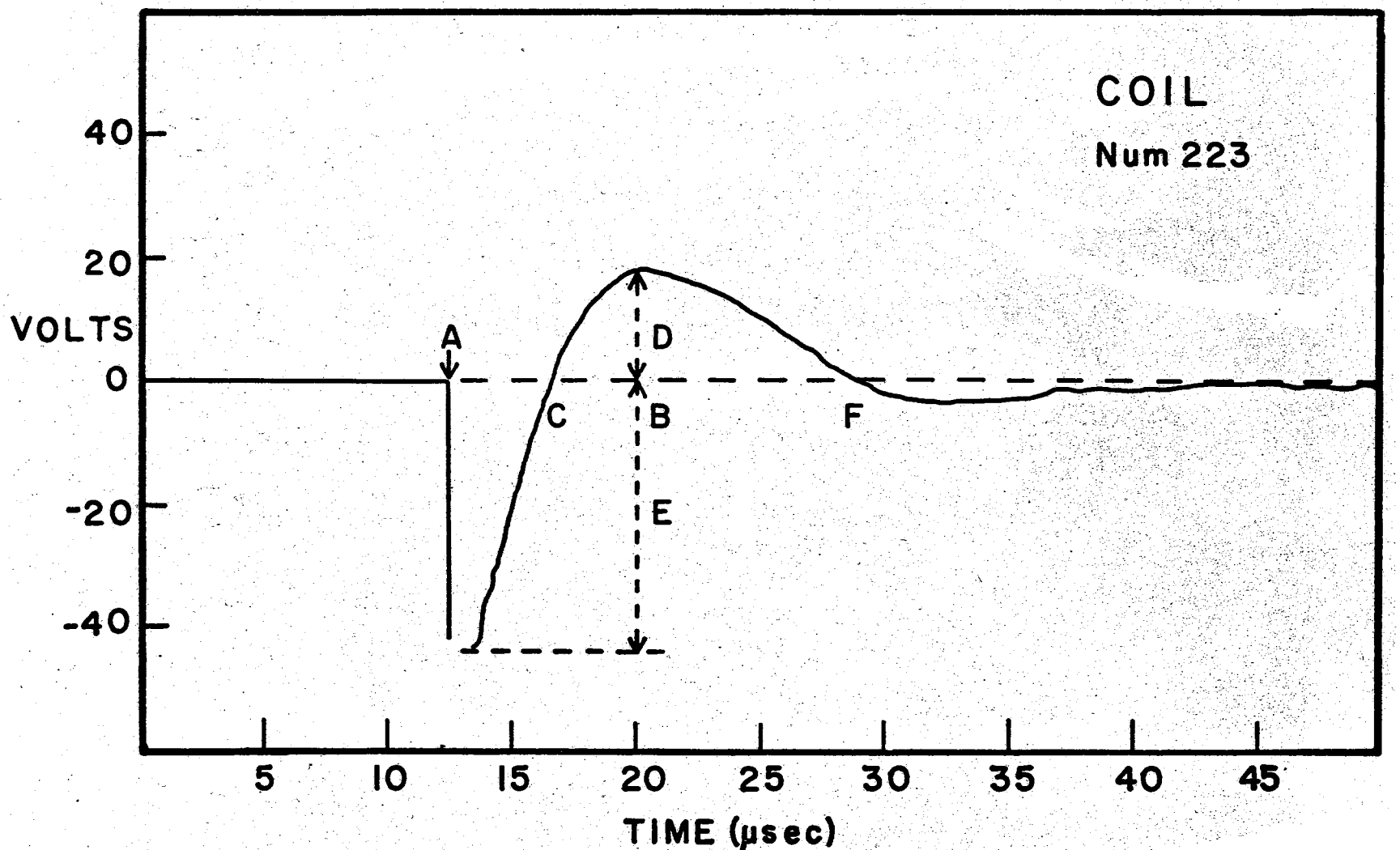

Figure 12. Current Derivative Pickup Coil Characteristics

$$\alpha t_1 = \frac{1}{2} \ln \frac{40 \text{ volts}}{18 \text{ volts}} \tag{3.20}$$

which yields

$$\alpha t_1 = 0.3987 \tag{3.21}$$

Thus

$$I_{max} = I_o e^{-(0.3987)}(0.8774) \tag{3.22}$$

where sin $\omega t = 0.8774$ from the previous discussion. Using the same I_o as before one gets

$$I_{max} = 3.69 \times 10^4 \text{ amps} . \tag{3.23}$$

Considering the assumptions made, this value is in good agreement with 3.17×10^4 amps calculated previously.

One should note that $dI/dt = 0$ at 4 μsec (point C), a value which is in agreement with Ross's[22] data. He reports current peaks occurring at 5 to 8 μsec. From Figure 12 one can see that the circuit is not critically damped but slightly underdamped with a minimum occurring at point F.

C. Results of Photodiode Measurement

Figure 13 illustrates the result of the photodiode output for the number 207 explosion. The photodiode is "looking" transverse to the wire through a black paper lined tube 1½ inches I.D. and 7 inches long. Thus, the SGD040 was 10 inches from the wire in the same plane as the wire. The total distance is 10 inches due to the 3 inches from the wall of the

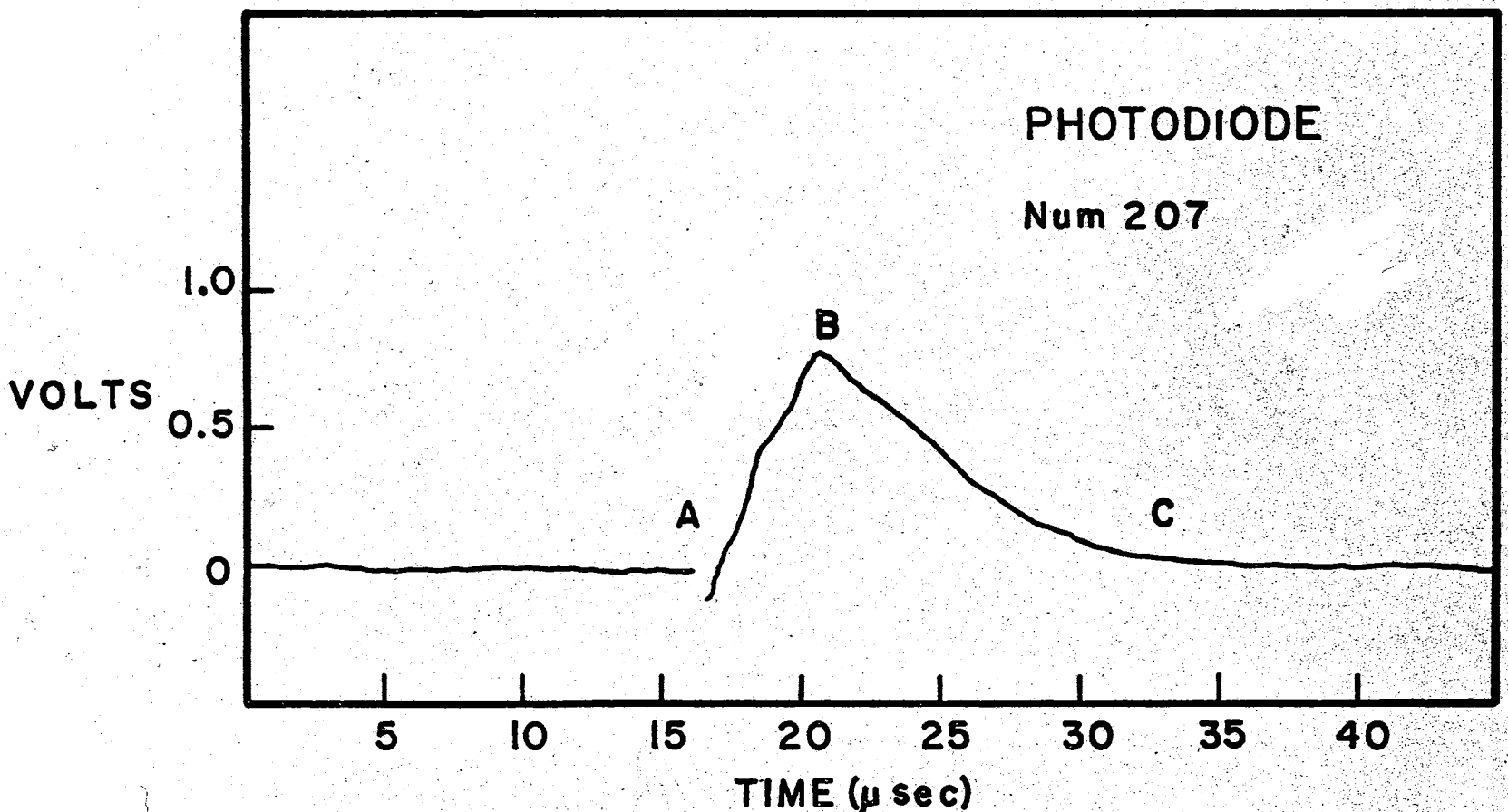

Figure 13. Photodiode Characteristics

pyrex vacuum chanber to the wire. One should notice the light from the plasma peaks at 4.5 μsec from point A, the point of ignition. From a comparison of Figure 12 with this figure one sees the light output reaches a maximum at about the same time as the current. Ross[22] measured the current and voltage simultaneously as a function of time. He found that the light intensity peaked at about the same time as a sudden drop in resistance occurred and theorized that this was the time for plasma production. The time for maximum current and maximum light output in this work were from 1 to 3 μsec less than those measured by Ross. However, in Ross's work, a No. 25 (0.0179 inches) wire was used whereas this work used No. 36 (0.005 inches) wire. The smaller wire could account for the time difference. The difference in the inductance between the two circuits could also cause the time difference. It should be noted that at 17 μsec (point C) the light signal is back to zero. On the basis of this observation and due to other data to be discussed later, it will be assumed the plasma has moved away from the wire by 17 μsec after ignition.

D. Results of Time-of-Flight Measurements

Figure 14 shows the previously discussed photodiode and dI/dt data. In addition, the ion flux data of the number 225 explosion is displayed. These data were taken with a 5 mil nickel wire exploded at 10 KV in a vacuum of 2.8×10^{-6} torr in a vacuum chamber containing only 1 detector. The possible origin of the first two data peaks will be discussed later in this chapter. Assuming point D, the third peak, is the positive ion flux going by the detector, the ion energy can be calculated by using $E = \frac{1}{2}mv^2$. The distance from point A, ignition, to point D, the

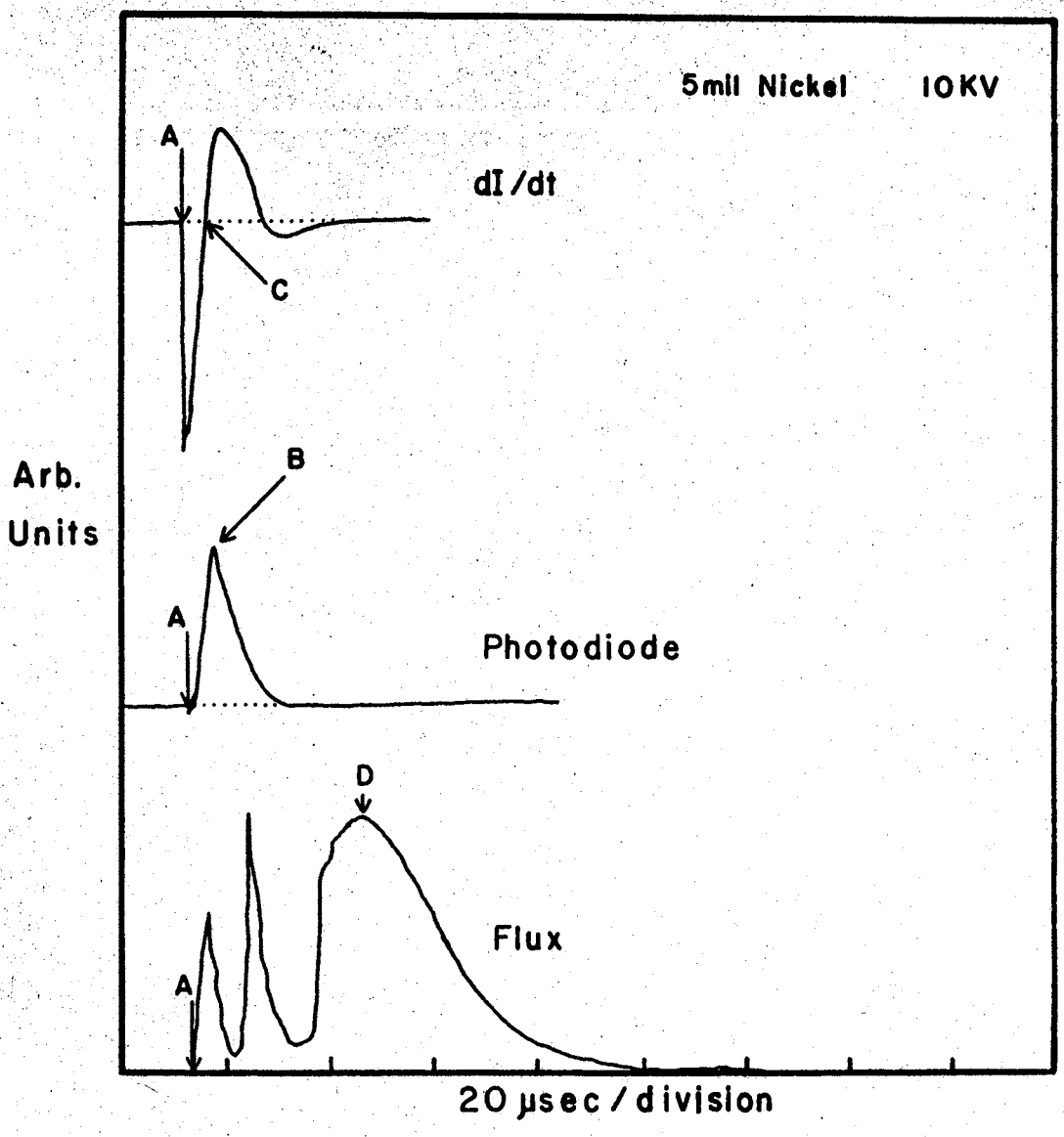

Figure 14. Pickup Coil, Photodiode, and Flux Characteristics

flux maximum, is 33 μsec. The photodiode response went to zero 17 μsec from ignition so it will be assumed this is when the plasma leaves the wire. Subtracting 17 μsec from 33 μsec yields 16 μsec for the flight time. The distance from the wire to the detector is 64.13 cm yielding a velocity of 4.0×10^{6} cm/sec. Taking the mass of a nickel ion to be 9.75×10^{-26} Kgm/atom one calculates an energy of 488.3 electron volts for the average energy of the ions. It will be seen later that this result is in complete agreement with data taken using 2 detectors which gives a more accurate measure of the velocity.

It was first thought that the first 2 peaks in the flux data of Figure 14 and other similar data were due to induced pickup from the high currents, from photo emission due to the intense light output, and soft x-rays. First an experiment was performed to determine the signal due to the pickup. At the point where the vacuum chamber reduces in size from 6 inches to 2 inches, the plasma was blocked off with a non-conducting stopper. It was discovered that the noise signal was less than 1 volt or on the order of 6% of the height of the first peaks in the data. This suggests that the first signals are due to more than pickup external to the plasma. Then an experiment was performed which showed that the initial signals in the data are due to the plasma itself. A 48 mm glass pipe was placed over the wire. This pipe was 4 feet long, hence it extended past the first detector but not past the second detector. The results are shown in Figure 15. Notice the bottom detector, Figure 15B, shows no appreciable signal. A somewhat typical signal appears at the second detector in Figure 15A. Thinking that perhaps the initial peaks were due to fast electrons, another experiment was performed. For the number 259 explosion a 1 kilogauss permanent magnet was

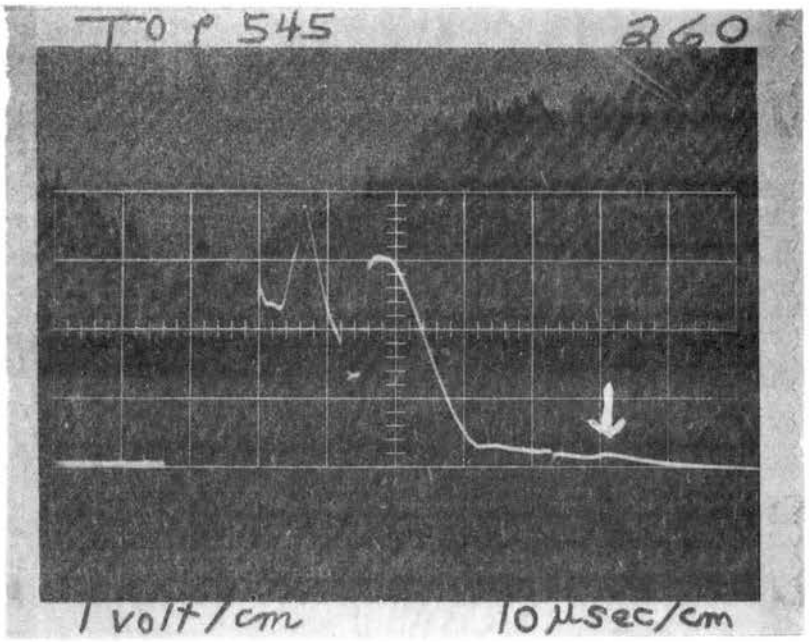

A

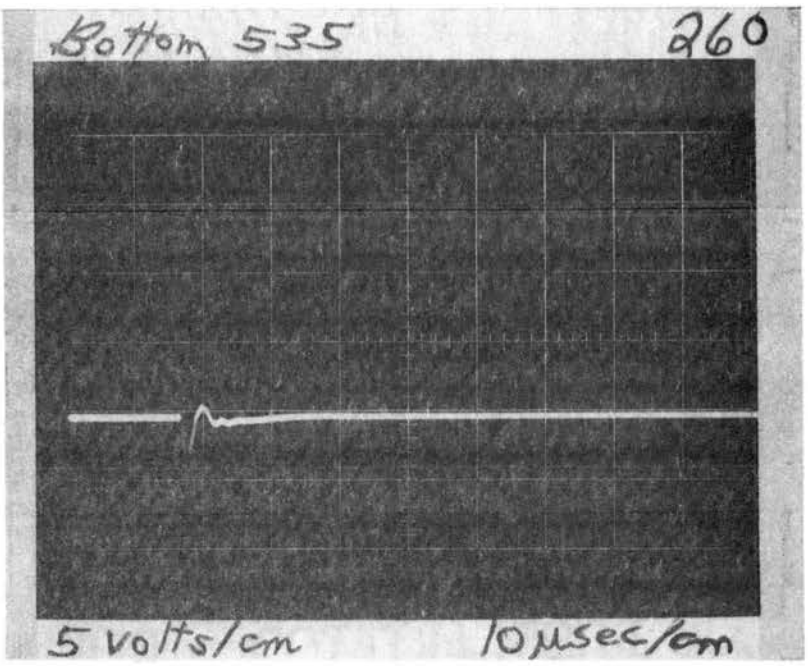

B

Figure 15. Photograph of Data From Explosion Number 260

placed 8 3/4 inches below the first detector such that the field was perpendicular to the axis of the pipe and the velocity vector of the plasma. The radius of curvature of the electrons would be

$$r = \frac{mv}{qB} \tag{3.24}$$

where m is the mass, v is the velocity, q the charge and B the magnetic field. Choosing a velocity of 10^7 cm/sec for the fast electrons

$$r = 5.69 \times 10^{-6} \text{ m} \tag{3.25}$$

Therefore, the magnetic field should stop the fast electrons. Figure 16 shows the first detector flux data of the number 258 explosion and the number 259 explosion. Both wires were 5 mil nickel blown at 10 KV in a vacuum of 3.1×10^{-6} torr and 1.8×10^{-6} torr respectively. Obviously the first peaks were not removed. However, the magnet data show a peak at B where one did not occur previously. The minimum C, in the non-magnet data, seems to be shifted to the right in time. The same thing can be said for the peak at E. The peak which is attributed to the positive ions (G and H) is shifted to the left in time in the magnet case. The detectors used in number 258 and 259 were 2 rings, one 90 mm in diameter and the other 80 mm in diameter. They differed from the previous detectors in that they are not wires protruding into the center of the chamber but rather circles just inside the chamber. Since these circles are at least 80 mm in diameter and the lower one is 15 inches above a 2 inch hole, X-rays or light could not directly strike the lower detector. However, the initial peak A might be due to photo emission caused by high intensity light scattered off the walls and striking the

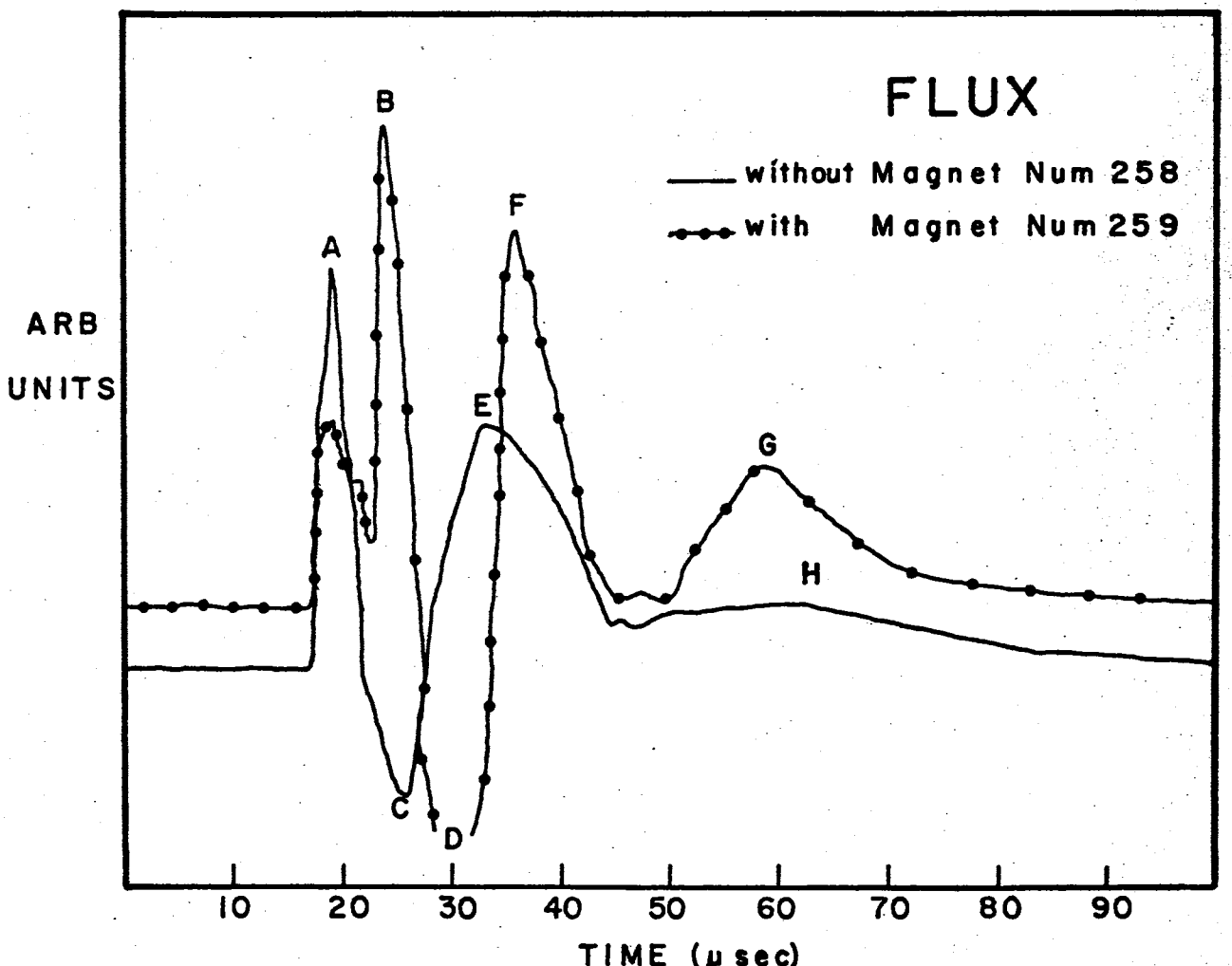

Figure 16. Magnetic Field Dependence of Flux Characteristics

copper detectors since this peak is not effected by the magnetic field. Any electrons getting to the detector in the time associated with point A would be low energy (2.7×10^7 cm/sec or 0.2 eV) hence peaks B, E, and F might be due to electrons which are effected by the magnetic field but not swept out by it. At best the initial peaks are due to a very complicated interaction which at present has no sound explanation.

Figures 17, 18, 19, and 20 are the results of flux measurements of the explosion numbers 247, 253, 258 and 259. The detectors for numbers 247 and 253 were described in Chapter II. The detectors for numbers 258 and 259 were as described previously in this section and Chapter II. In each case point A was the time considered for the positive ions to pass the first detector and point B is the time considered for the ions to pass the second detector. Table I displays the results as analyzed for these three explosions. The average ion energy for the first three explosions is in good agreement with Ross's data. The complex interaction of the plasma may account for the results of explosion number 259 where the magnet was used. Figure 21 shows a plot of time from ignition versus distance from wire for the two detectors. One should notice that all three curves extrapolate close to 17 μsec, the chosen plasma release time in the analysis of number 225. Also the energies are in good agreement between the one detector and the two detector analysis.

Wires of nine different elements have been exploded in this work. Figure 22 shows the one detector flux results from explosions number 189, 192, 193, and 194. Figure 23 shows the result from explosions 190, 191, 195, 197, and 198. The elements of the various explosions are labeled in the figures. Two groups of data are formed from the different elements. Table II shows the electronic configuration for these 9

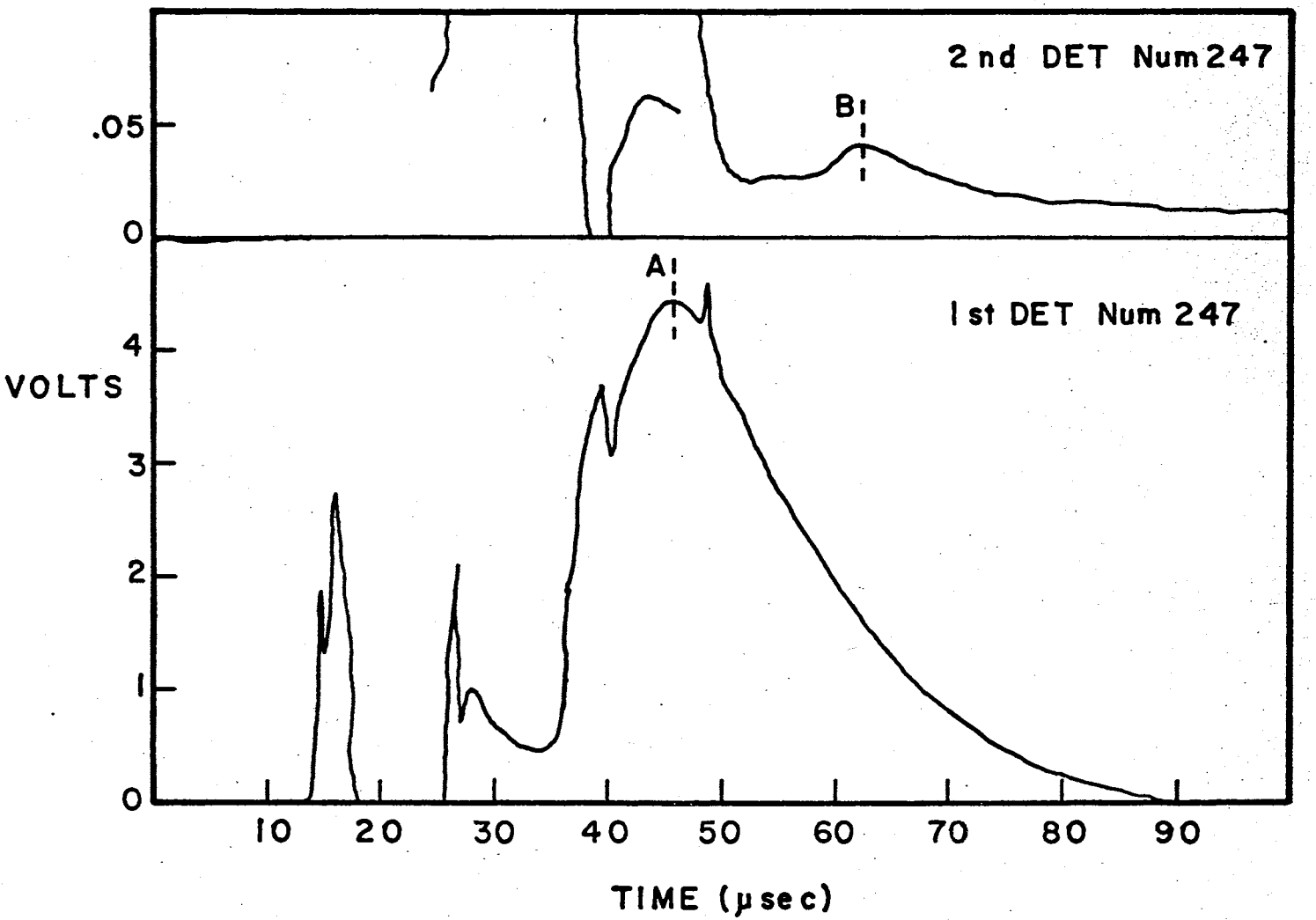

Figure 17. Flux Characteristics of Explosion Number 247

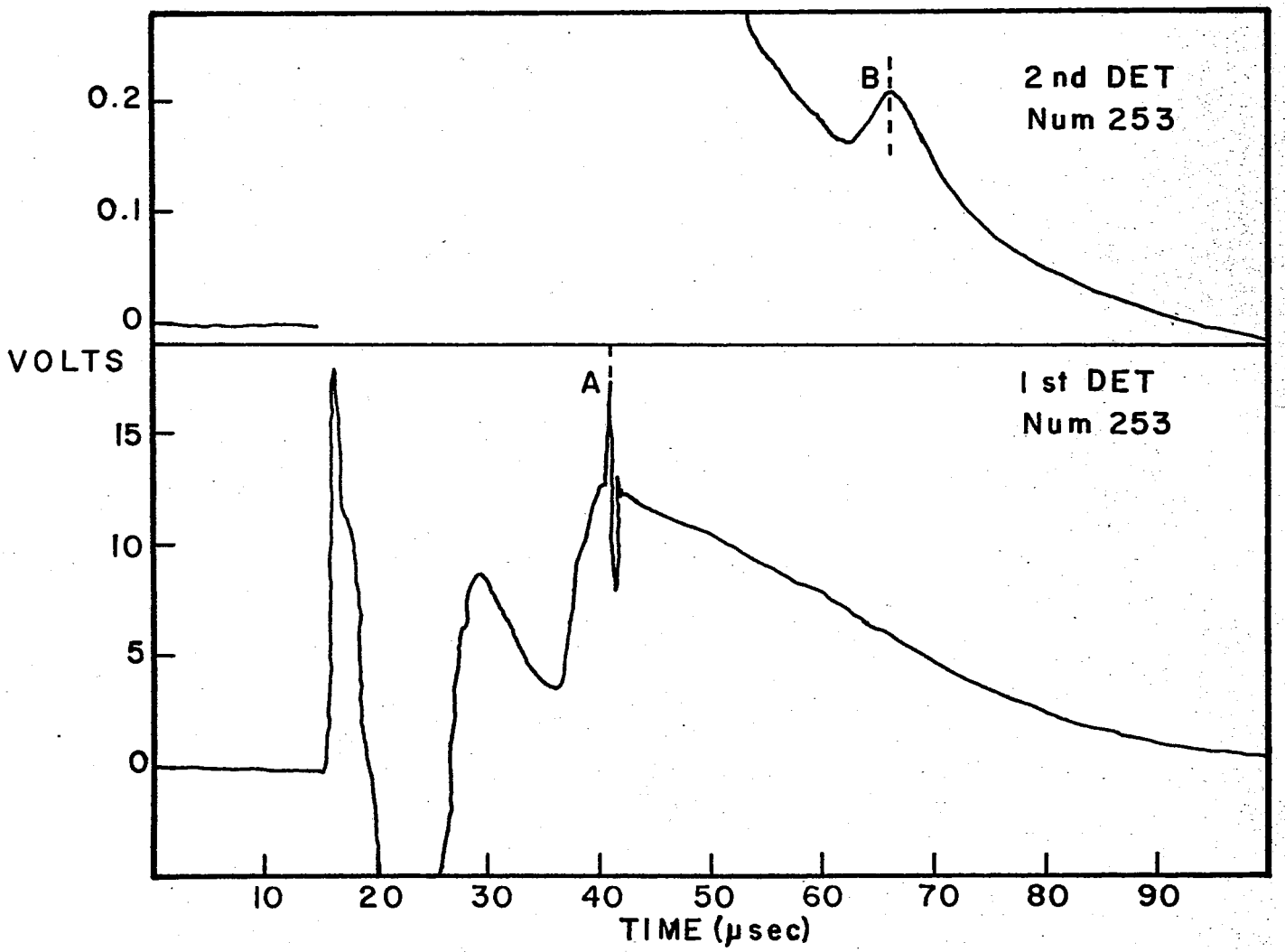

Figure 18. Flux Characteristics of Explosion Number 253

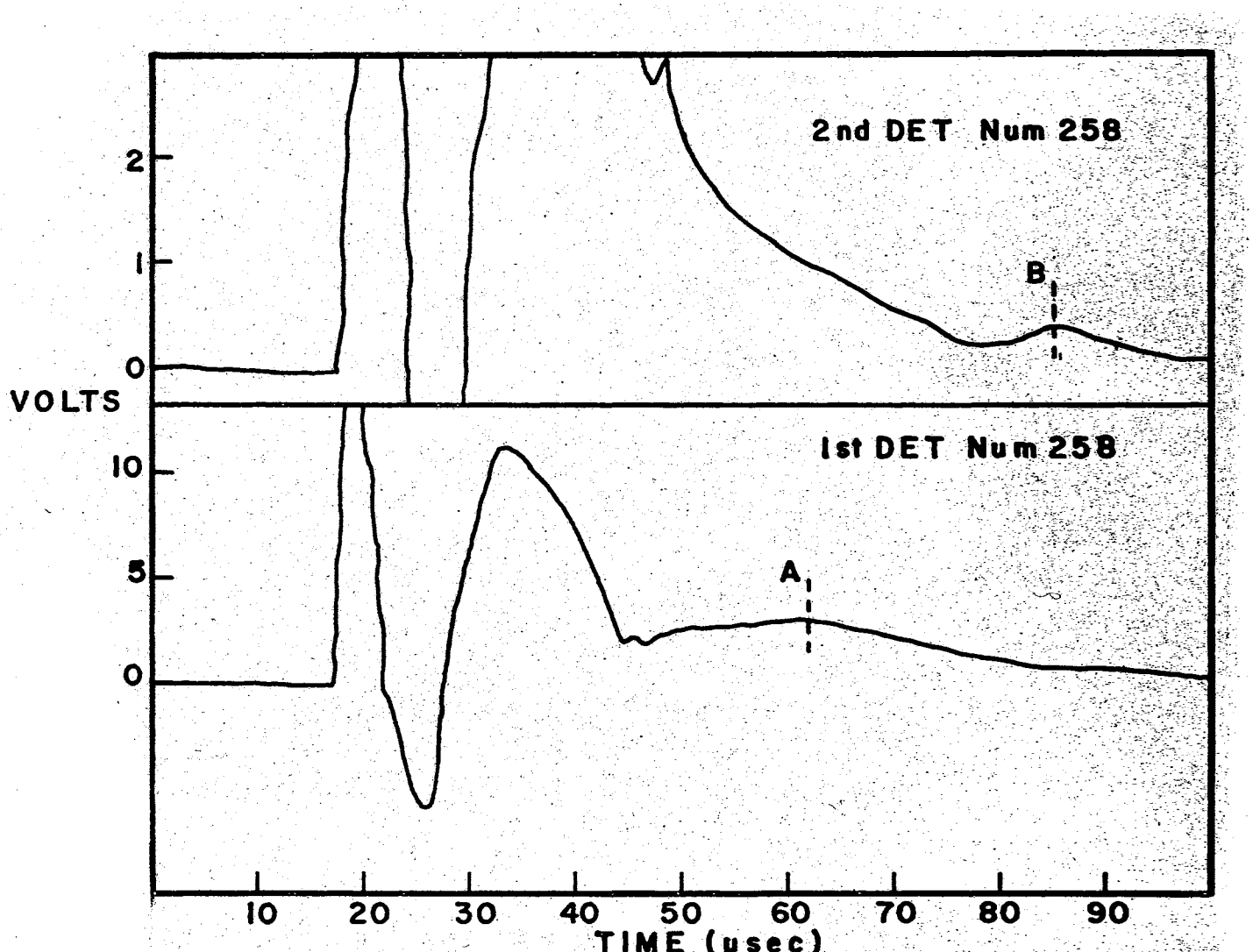

Figure 19. Flux Characteristics of Explosion Number 258

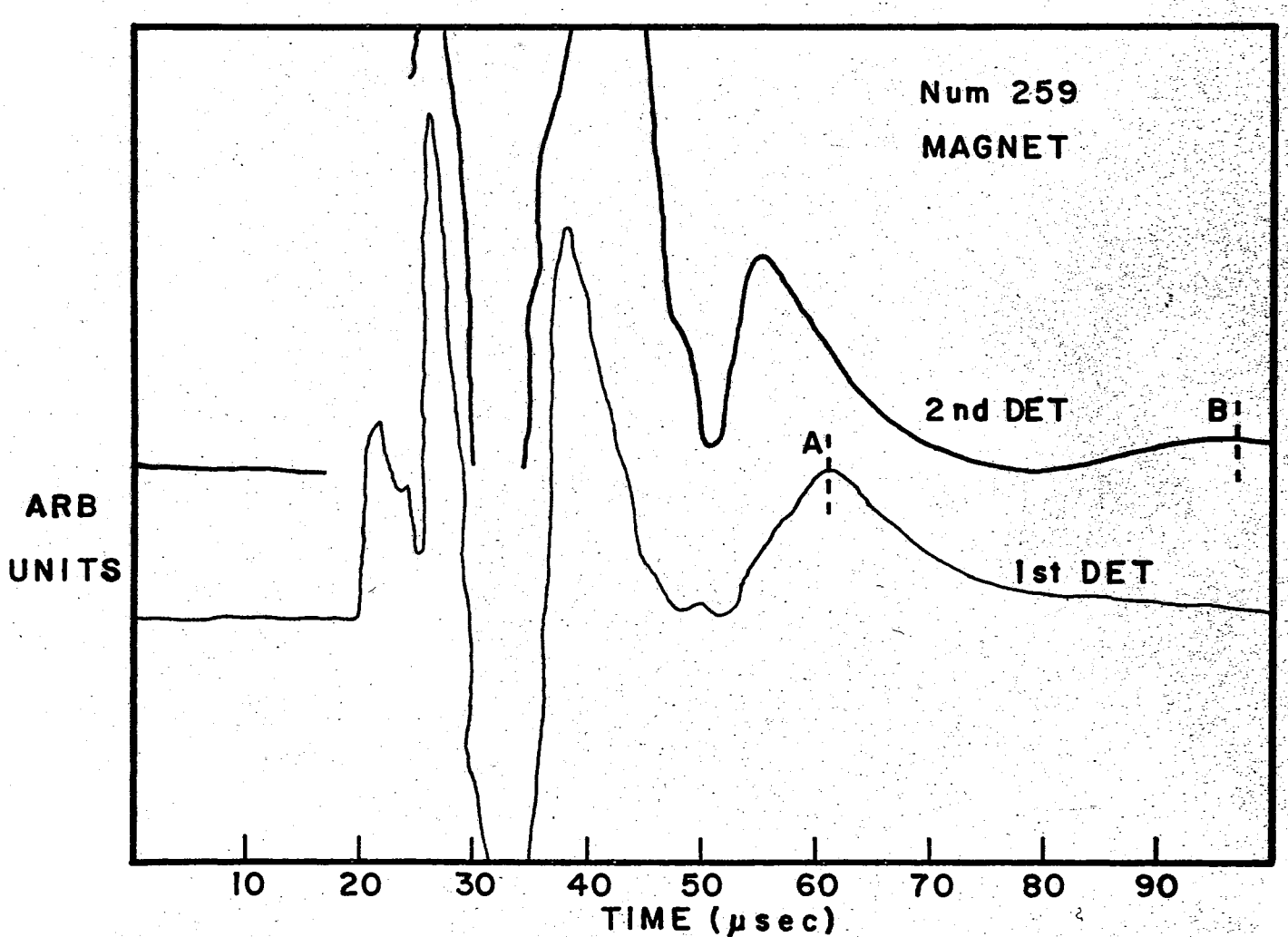

Figure 20. Flux Characteristics of Explosion Number 259

TABLE I

TABULATION OF ION ENERGIES

Explosion Number	Vacuum	Distance Difference	Time Difference	Velocity	Energy
#247	1.9×10^{-6} torr	85 cm	17 μsec	5.0×10^{6} cm/sec	761.5 ev
#253	2.4×10^{-6} torr	85 cm	25 μsec	3.4×10^{6} cm/sec	352.1 ev
#258	3.1×10^{-6} torr	91.44 cm	23 μsec	3.98×10^{6} cm/sec	482 ev
#259 MAGNET	1.8×10^{-6} torr	91.44 cm	36 μsec	2.54×10^{6} cm/sec	196.5 ev
#247, #253, #258	Average		Energy	531.86 ev	
#247, #253, #258	Average		Velocity	4.12×10^{6} cm/sec	

Wire: Nickel (5 mil) Voltage: 10 KV Energy = $\frac{1}{2}$ mv^2

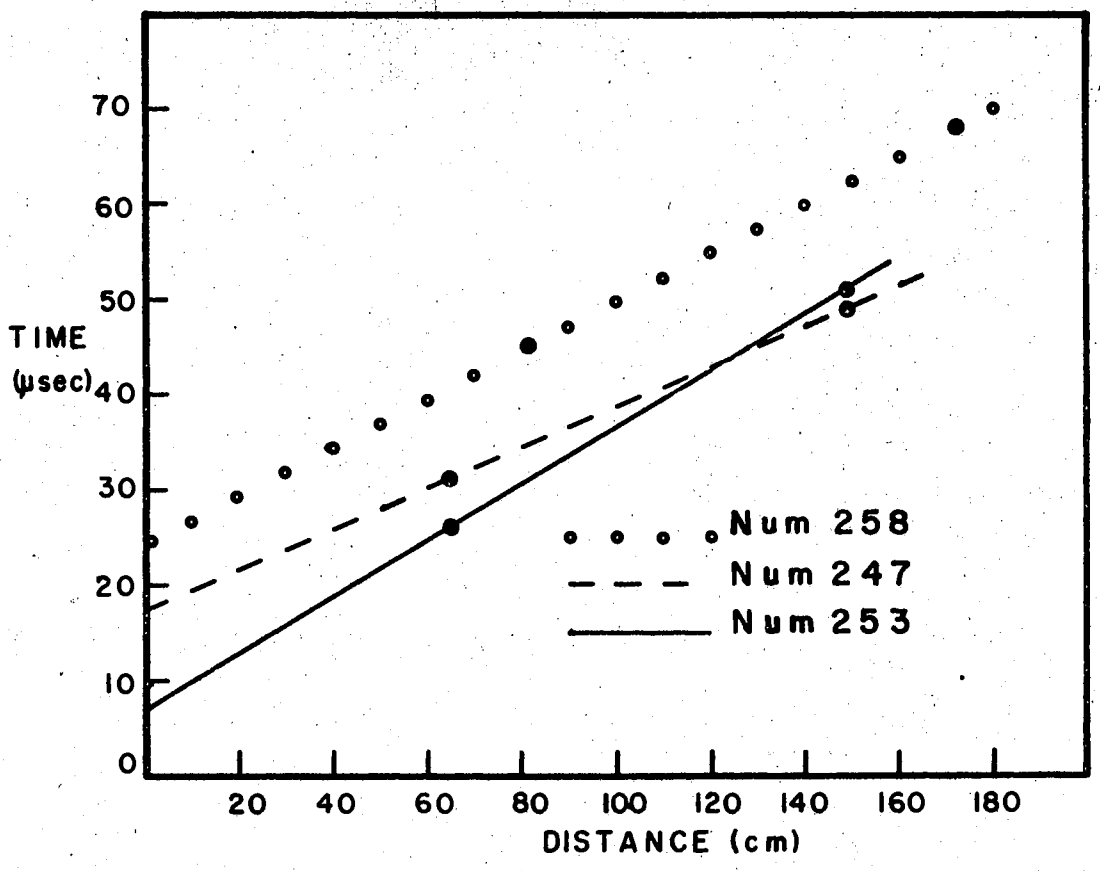

Figure 21. Time From Ignition as a Function of Distance From Wire

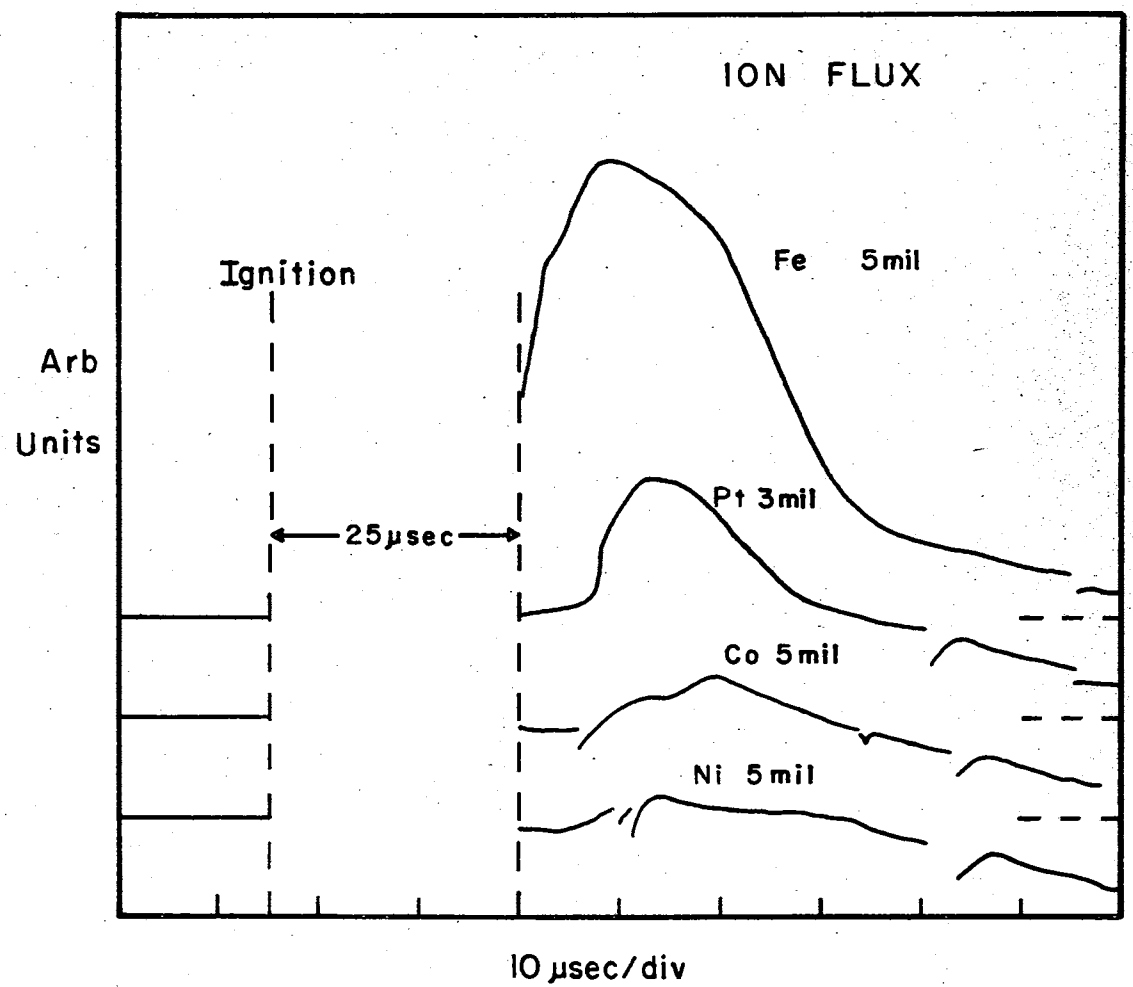

Figure 22. Ion Flux Characteristics of the First Four Elements of Table II

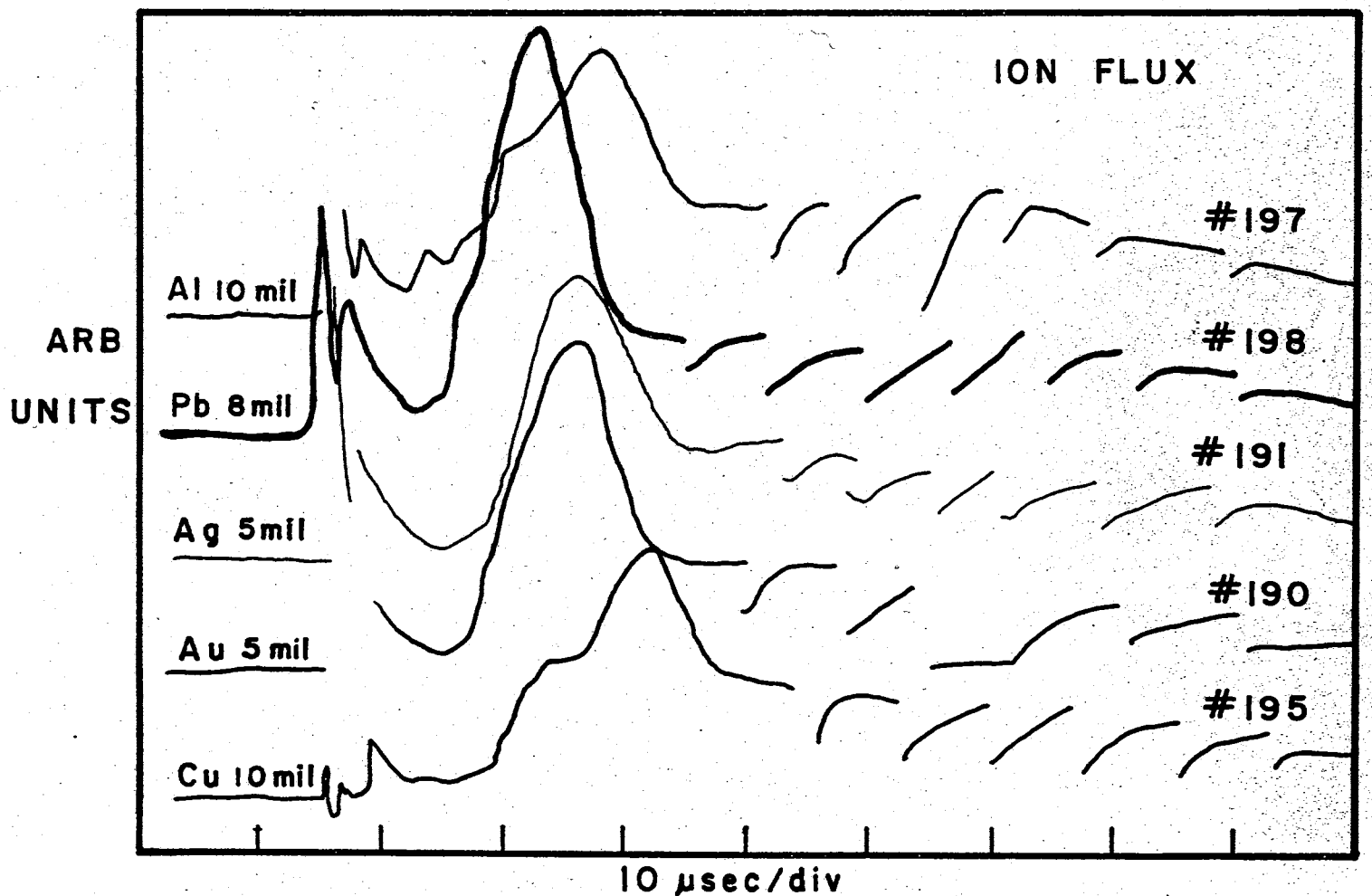

Figure 23. Ion Flux Characteristics of the Last Five Elements of Table II

TABLE II

ELECTRONIC CONFIGURATION

Element	At. No.	K	L	M	N	O	P
		s	s p	s p d	s p d f	s p d f	s p d f
Iron	26	2	2 6	2 6 6	2		
Platinum	78	2	2 6	2 6 10	2 6 10 14	2 6 9	1
Cobalt	27	2	2 6	2 6 7	2		
Nickel	28	2	2 6	2 6 8	2		
Aluminum	13	2	2 6	2 1			
Gold	79	2	2 6	2 6 10	2 6 10 14	2 6 10	1
Silver	47	2	2 6	2 6 10	2 6 10 1		
Copper	29	2	2 6	2 6 10	1		
Lead	82	2	2 6	2 6 10	2 6 10 14	2 6 10	2 2

elements. The elements of the wires for the data in Figure 22 have an unfilled d shell. Those used for the data shown in Figure 23 have all but the last shell filled. The electronic configuration is the only correlation that can be made between the two groups of elements. It should be noted that when a conducting plate was placed immediately below the top plexiglas plate and was grounded, the chopped oscillations shown in Figure 23 disappeared. Thus the oscillations are probably due to electrons or the positive ions interacting with electrons at the top plate. When the capacitor voltage was decreased the elements of Figure 22 showed a pattern similar to Figure 23. Thus it is strongly believed that the available energy and hence the energy put into the wire greatly effects the ionization. Furthermore, the nine elements fit into one group or another because of their particular energy requirement. In fact, the element with the lowest second ionization state (iron) has the largest flux magnitude.

The density of the ions was determined to be 1.74×10^{15} ion/cm^3. This number was determined in the following way. The total charge passing the detector was obtained by integrating the area under the positive ion peak for the explosion number 247, Figure 17. The maximum current was determined by dividing 4.5 volts, the signal height, by 50 ohms, the load resistor. This yields a current of 90 ma. The base of the triangle approximating the area under curve A is 35 μsec; thus 1/2 (35 μsec) (90 ma) = 1.57×10^{-6} coul. Dividing this number by 1.6×10^{-19} coul/ion (assuming singly ionized particles) yields 9.8×10^{12} ions. The total area of the detectors is 0.292 cm^2 and the total area of the pipe is 45.36 cm^2. So from the following relation

$$\frac{9.8 \times 10^{12} \text{ ion}}{.292 \text{ cm}^2} = \frac{x \text{ ions}}{45.36 \text{ cm}^2}$$

one gets the total number of ions = 1.52×10^{15} ions. Now if one assumes that only 1/1000 of the particles interact with the detector, due to the fact the detectors do not extend into the mainstream of the plasma beam, the number of ions passing the detector is assumed to be $\approx 10^{18}$ ions. Since one wire of 5 mil nickel 1 cm long constains 1.14×10^{19} atoms this is on the order of 10% of the available atoms. A volume of a plasma slug was calculated based on the velocity and pulse width. The velocity is 5×10^{6} cm/sec and the pulse width is 35 μsec yielding a length of 175 cm. The pipe cross section is 45.36 cm^2 so the volume is 7938 cm^3. Now 1×10^{18} ions/7.938×10^{3} cm^3 yields a density of 1.91×10^{14} ions/cm^3. Because of this particular velocity and the assumptions made, it is felt that this density is low by at least 3 orders of magnitude. It does give some rough idea of the densities involved.

CHAPTER IV

SUMMARY AND SUGGESTIONS FOR FUTURE STUDY

An exploding wire ion generator has been designed and studied. The device is built around a capacitor bank and Lovotron switch. When energy is released into a wire it explodes creating a plasma with ion densities on the order of 10^{14} to 10^{18} ions/cm^3. The peak current during the capacitor discharge is on the order of 10^4 amps.

It is immediately apparent that the plasma from exploding wires is complicated and does not lend itself to a simple explanation. It was found that the ions could be detected and their energy measured to within a factor of 2 from one explosion to the next. The energy for the ions ranged from 352 electron volts to 762 electron volts with an average of 531 electron volts. It appears that the geometry of the plasma chamber plays an important role in determining the plasma characteristics.

The origin of the initial peaks in the flux data was studied extensively. One can list three possible origins for these peaks. One is the inductive cross talk in the circuitry. Through a series of experiments this source was eliminated meaning that these peaks must be due to some internal mechanism. An experiment using a glass pipe to bypass the first detector suggests the peaks are due to particles within the plasma. These particles could be electrons generated by the wire explosion itself or electrons removed from the detectors by soft X-rays and photo emis-

sion. The experiment using the magnetic field below the first detector suggests that the peaks may be due to high energy electrons which interact with but are not swept out by the magnetic field.

In the future, further study needs to be made to determine the origin of the initial peaks. This can be done by using commercially available solid state detectors. Solid state detectors can also be used to measure the density and energy of the positive ions. The positive ions must be accelerated before implantation can occur. The extraction of positive ions by various shapes of electrodes and containers surrounding the explosion can be tried. Better control of the circuit parameters, inductance, resistance and charge is necessary to see if the energy spread measured in this work can be eliminated.

It is felt that this work indicates an exploding wire is a feasible source for use in ion implantation studies. It is an inexpensive method of readily attaining a high density beam of analyzable positive ions from solid conducting materials. Wires of some 15 different elements have been obtained with analysis of these elements to take place in the immediate future.

The results and data presented here represent a small amount of the data taken. Some 260 wires were exploded over a period of one year. This work is a brief description of the project and the results rather than a catalog of all the results.

BIBLIOGRAPHY

1. Woolf, M., and Reif, F., "Effect of Magnetic Impurities on the Density of States of Superconductors", Physical Review, 137, A557 (1965).

2. Matthias, B. T., Suhl, H., and Corenzivit, E., "Spin Exchange in Superconductors", Phys. Rev. Letters, 1, 92 (1958).

3. Wick, G. L., "Ion Implantation", Science, 170, 425 (23 October 1970).

4. Thompson, S. A., "Ion Implantation", The Electronic Engineer, 28, 68 (January 1969).

5. Kleinfelder, W. J., Properties of Ion-Implanted Boron, Nitrogen, and Phosphorus in Single-Crystal Silicon, Stanford Electronic Laboratories, Technical Report No. K701-1 (March 1967).

6. Vook, F. L., and Stein, H. J., "Evidence for Vacancy Motion in Low Temperature Ion-Planted Si", Radiation Effects, 6, 11 (1970).

7. Buckel, W., et. al., "Superconductivity of Pb- and Sn-Films After Implantation of Mn-Ions", Zeitschrift fur Physik, 245, 283 (1971).

8. Borders, J. A., and Brower, K. L., "EPR of Substitutional Group V Implants in Silicon", Radiation Effects, 6, 135 (1970).

9. Crocknell, P. J., Gettings, M., and Stephens, K. G., "Use of Low-Energy Accelerators for Ion Implantation", Nuclear Instruments and Methods, 92, 465 (1971).

10. Brice, D. K., "Ion Implantation Depth Distributions: Energy Deposition into Atomic Processes and Ion Locations", Appl. Phys. Letters, 16, 103 (1970).

11. Perkins, J. G., and Collins, L. E., "Resistive Layers Formed by Ion Implantation into Metal Films", Thin Solid Films, 5, R59 (1970).

12. Mayer, J. W., Eriksson, L., and Davies, J. A., Ion Implantation in Semiconductors, Academic Press, New York, N. Y., (1970).

13. Gibbons, J. F., "Ion Implantation in Semiconductors - Part I Range Distribution Theory and Experiments", Proceedings of the IEEE, 56, 295 (1968).

14. Chace, W. G., "A Brief Survey of Exploding Wire Research", Exploding Wires Volume I, W. G. Chace and H. K. Moore, ed., Plenum Press, New York, N. Y. (1959), p. 7.

15. Chace, W. G., and Moore, H. K., editors, Exploding Wires Vol. I, Plenum Press, New York, N. Y. (1959).

16. Chace, W. G., and Moore, H. K., editors, Exploding Wires Vol. II, Plenum Press, New York, N. Y. (1962).

17. Chace, W. G., and Moore, H. K., editors, Exploding Wires Vol. III, Plenum Press, New York, N. Y. (1964).

18. Chace, W. G., and Watson, E. M., A Bibliography of the Electrically Exploded Conductor Phenomenon, Fourth Edition, Air Force Cambridge Research Laboratories, Report No. AFCRL-67-0556 (October 1967).

19. Vlastos, Antonios, "Restrike Channel Resistance of Thin Exploding Wires", J. of Appl. Phys., 40, 4752 (1969).

20. Langworthy, J. B., et. al., Electrically Exploded Wires - Experiments and Theory, Naval Research Laboratory, Progress Report - 7/III/58 to 30/VI/60, NRL Report No. 5489 (1961).

21. Bennett, F. D., Kahl, G. D., and Wedemeyer, E. H., "Resistance Changes Caused by Vaporization Waves in Exploding Wires", Exploding Wires Vol III, W. G. Chace and H. K. Moore, ed., Plenum Press, New York, N. Y. (1964), p. 65.

22. Ross, D. P., "Positive Ion Heating of Plasmas Produced From the Solid State", Ph.D. Thesis, University of Arkansas, University Microfilms, Inc., Ann Arbor, Michigan (1967).

23. Ross, D. P., and Zinke, O. H., "High-Temperature Plasmas Produced by Exploding Wires", Exploding Wires Vol IV, W. G. Chace and H. K. Moore, ed., Plenum Press, New York, N. Y. (1968), p. 147.

24. Erb, W., and Calker, J. V., "Exploding Wires of Ni, Mo, and W", Zeitschrift fur Angewandte Physik, 31, 71 (1971).

25. Oktay, E., "Effect of Wire Cross Section on the First Pulse of an Exploding Wire", Rev. of Sci. Inst. 36, 1327 (1965).

26. Arzimovich, L. A., Elementary Plasma Physics, Blaisdell Pub. Co., New York, N. Y. (1965).

27. McWhirter, R. W. P., "Spectral Intensities", Plasma Diagnostic Techniques, R. H. Huddlestone and S. L. Leonard, ed., Academic Press, New York, N. Y. (1965), p. 258.

28. Rusbridge, M. G. and Wort, D. J. H., "Comparison of Microwave

Transmission and Langmuir Probe Methods of Measuring Plasma Density", Plasma Physics, 9, 239 (1967).

29. Chen, Francis F., "Electric Probes", Plasma Diagnostic Techniques, R. H. Huddlestone and S. L. Leonard, ed., Academic Press, New York, N. Y. (1965), p. 113.

30. Mott-Smith, H. M. and Langmuir, Irving, "The Theory of Collectors in Gaseous Discharges", Phys. Rev., 28, 727 (1926).

31. Huddleston, Richard H. and Leonard, Stanley L., ed., Plasma Diagnostic Techniques, Academic Press, New York, N. Y., (1965).

32. Chen, F. F., "Double-Probe Method for Unstable Plasma", The Rev. of Sci. Inst., 35, 1208 (1964).

33. Chapuk, J. M., et. al., "Probe System for Plasma Research", The Rev. of Sci. Inst., 34, 1377 (1963).

34. Boyd, R. L. F., "The Collection of Positive Ions by a Probe in an Electrical Discharge", Proc. Royal Soc. of London Series A, 201, 22 (1950).

35. Lindberg, L. and Kristoferson, L., "Electric Probe Measurements in a Moving and Magnetized Plasma", Plasma Physics, 12, 831 (1970).

36. Peterson, E. W. and Talbot, L., "Langmuir Probe Response in a Turbulent Plasma", AIAA Journal, 8, 1391 (1970).

37. Cooney, J. A., "Method of Measuring the Velocity of a Continuously Flowing Plasma", The Rev. of Sci. Inst., 35, 442 (1964).

38. de Boer, P. C., "Probe for Measuring Ion Density in Slightly Ionized High Speed Flow", The Rev. of Sci. Inst., 37, 775 (1966).

39. Nielsen, K. O., "The Development of Magnetic Ion Sources for an Electromagnetic Isotope Separator", Nuclear Instruments, 7, 289 (1957).

40. Almén, O. and Nielsen, K. O., "Systematic Investigation of a Magnetic Ion Source for an Electromagnetic Isotope Separator", Nuclear Instruments, 7, 302 (1957).

41. Magnuson, G. D., et. al., "High Efficiency Source for Metal Ions", The Rev. of Sci. Inst., 36, 136 (1965).

42. Brown, G. and Renton, M. L., "Performance of a Sputter Ion Source and its Application for Implanted Ion Profile Experiments", Nuclear Instruments and Methods, 92, 477 (1971).

43. Krimmel, E. F., "Universal High Current Ion Source for Ions From Solids", Zeitschrift fur Angewandte Physik, 31, 51 (1971).

44. Wilson, R. G., "Ion Implantation Sources", International Conference on Applications of Ion Beams, Philippe Glotin, ed., Gap Editions Ophrys, Grenoble, France (1967), p. 105.

45. Livingston, M. S. and Blewett, J. P., Particle Accelerators, McGraw-Hill Book Co., New York, N. Y. (1962).

46. Cullington, E. H., Chace, W. G. and Morgan, R. L., Lovotron-A Low Voltage Triggered Switch Gap, Air Force Cambridge Research Laboratories, Report No. AFCRC-TR-55-227 (1955).

47. Duerksen, K. D., Walker, R. L., and Karioris, F. G., "Exploding-Wire Aerosol Generator", Health Physics Division Annual Progress Report, Oak Ridge National Laboratory, Report No. ORNL-4168 (October 1967), p. 296.

48. Boley, F. I., Plasmas-Laboratory and Cosmic, D. Van Nostrand Co., Inc., Princeton, New Jersey (1966).

VITA

Kenneth Dean Duerksen

Candidate for the Degree of

Master of Science

Thesis: AN EXPLODING WIRE ION SOURCE FOR ION IMPLANTATION

Major Field: Physics

Biographical:

Personal Data: Born in Cordell, Oklahoma, December 13, 1943, the son of Erwin R. and Luella H. Duerksen.

Education: Graduated from Corn High School, Corn, Oklahoma, in May, 1962; received the Bachelor of Science degree in physics from Southwestern State College, Weatherford, Oklahoma, in May, 1966; enrolled in the master's program at the University of Arkansas, 1966 - 1967; completed requirements for the Master of Science degree at Oklahoma State University in May, 1972.

Professional Experience: Undergraduate Laboratory Teaching Assistant, Southwestern State College, 1964 - 1966; Research Technician, Oak Ridge National Laboratory, Summer 1966; Graduate Teaching Assistant, Department of Physics, University of Arkansas, 1966 - 1967; Instructor of Physics, Westark Junior College, Fort Smith, Arkansas, 1967 - 1969; Graduate Teaching Assistant, Department of Physics, Oklahoma State University, 1969 - 1971; Graduate Research Assistant, Department of Physics, Oklahoma State University, 1971 - 1972.

Professional Organizations: Associate Councilor from Zone 10 on the National Council of the Society of Physics Students, the SPS, Sigma Pi Sigma National Physics Honor Society, The American Association of Physics Teachers.

Publications: "Exploding-Wire Aerosol Generator", Health Physics Division Annual Progress Report, Oak Ridge National Laboratory, Report No. ORNL-4168 (October 1967), p. 296.